The Great Equalizer: Medicare and the Geography of Consumer Financial Strain*

Paul Goldsmith-Pinkham† Maxim Pinkovskiy‡ Jacob Wallace§

January 31, 2021

Abstract

We use a five percent sample of Americans' credit bureau data, combined with a regression discontinuity approach, to estimate the effect of universal health insurance at age 65—when most Americans become eligible for Medicare—at the national, state, and local level. We find a 30 percent reduction in debt collections—and a two-thirds reduction in the geographic variation in collections—with limited effects on other financial outcomes. The areas that experienced larger reductions in collections debt at age 65 were concentrated in the Southern United States, and had higher shares of black residents, people with disabilities, and for-profit hospitals.

*First version: April 22, 2017. This version: January 31, 2021. The views expressed are those of the authors and do not necessarily reflect those of the Federal Reserve Bank of New York or the Federal Reserve System. The authors would like to thank Neale Mahoney, Matt Notowidigdo, Chima Ndumele, Mark Schlesinger, Julia Smith, Isaac Sorkin, Eric Zwick, and Trevor Gallen for helpful comments along with participants at the BU, Harvard, MIT Health Economics Seminar; Yale SOM Finance Lunch; Association for Public Policy Analysis and Management; Gerzensee European Summer Symposium in Financial Markets; NTA Annual Conference on Taxation; and Salomon Center/BPI Conference on Household Finance. Joseph Doran, Danno Lemu, Davy Perlman, and Lauren Thomas provided excellent research assistance.

†Yale School of Management. Email: paul.goldsmith-pinkham@yale.edu

‡Federal Reserve Bank of New York. Email: maxim.pinkovskiy@ny.frb.org

§Yale School of Public Health. Email: jacob.wallace@yale.edu

1 Introduction

Why does consumer financial strain vary so much across the United States (Keys, Mahoney and Yang, 2020)? In this paper, we examine the role that health insurance plays in shaping the geography of financial health. To do this, we use a five percent sample of Americans' credit report data, combined with a regression discontinuity (RD) approach, to estimate the effect of universal health insurance at age 65—when most Americans become eligible for Medicare—at the national, state, and commuting zone level.

We use our location-specific estimates of Medicare's effects for three purposes. First, we show that Medicare reduces geographic variation in debt collections by two-thirds at age 65. Second, we show that the gains in financial health due to Medicare are greatest in the South, where a higher share of the near-elderly (i.e., 55-64 year olds) are uninsured and the financial health improvements *per newly-insured individual* are largest. We show that the commuting zones (CZs) experiencing the largest gains in financial health at age 65 had larger shares of black residents, people with disabilities, and for-profit hospitals. Third, using shrinkage estimators, we construct forecasts of the causal effect of expanding coverage to the near-elderly in each of the 741 CZs in the United States, which we use to evaluate existing policies and potential future expansions.

To quantify how Medicare reduces geographic disparities in consumer financial strain, we construct counterfactual estimates of consumer financial outcomes at age 65, with and without Medicare, for each locality. With these location-specific counterfactuals, we construct an estimator of the nationwide, cross-locality reduction in the *variance* of consumer financial outcomes. Using this approach, we show that Medicare reduces the geographic variation in collections by two-thirds at age 65, highlighting an understudied aspect of the Medicare program—that it largely eliminates geographic disparities in access to insurance (which fall by 93.5% at age 65), and substantially reduces geographic disparities in collections-related financial strain. However, we do not find evidence that Medicare reduces geographic variation in the other financial health outcomes we study (e.g., credit score, bankruptcy, delinquent debt), though our confidence intervals are quite wide.

Second, we explore why the effect of Medicare on collections debt, where we find a large reduction in geographic variation, differs so much across localities. We find that reductions in

collections debt are higher in areas that experienced larger increases in the insurance rate at age 65, suggesting that the gains in financial health are primarily driven by reducing the number of uninsured, rather than changes in the composition of coverage.[1] Motivated by this finding, we then examine how CZ-level reductions in collections differ between areas on a per capita and per newly-insured basis, with the latter done by scaling the change in financial health estimates by the estimated effect of Medicare on insurance rates. While our analysis suggests that a *primary* mechanism through which Medicare affects financial strain is by reducing the uninsurance rate, it is unlikely that the exclusion restriction holds.[2] As a result, we view this as an informative scaling exercise rather than an estimate of the causal effect of health insurance coverage on debt collections. To understand why the effects of Medicare differ across areas, we examine the demographic and healthcare market characteristics associated with the 741 causal estimates of CZ-level reductions in per capita collections debt at age 65. We find that the effect of Medicare on collections debt is larger in areas with larger shares of black residents, people with disabilities, and for-profit hospitals.

Third, we construct forecasts of the causal effect of Medicare on financial health in each CZ. This gives us a local approximation to the effect of lowering the Medicare eligibility age, a popular policy proposal. To reduce noise, we follow Chetty and Hendren (2018) and construct forecasts using a shrinkage estimator that combines our unbiased RD estimates and a predicted effect for each CZ based on its demographic and healthcare market characteristics. Maps of the forecast reductions in per capita and per newly-insured debt collections are strikingly similar, with the largest values in both concentrated in the South. For example, a coverage expansion to the near-elderly is forecast to reduce collection balances by 53 dollars per capita in Raleigh, NC (one of the largest forecast reductions). In contrast, the same treatment in San Francisco, CA, is only forecast to reduce collection balances by 8 dollars per capita. This is not simply because there are a greater share of uninsured in Raleigh; in fact, the near-elderly uninsurance rates in the two places are

[1] Our state-level results imply a reduction in collection balances of $584 per newly-insured individual at 65, which falls within the range of estimates from prior work on the effects of Medicaid coverage (Finkelstein et al., 2012; Hu et al., 2018).

[2] For individuals with no insurance prior to Medicare, turning 65 provides a big increase in risk protection. However, for individuals with insurance at age 65, the transition to Medicare changes premiums, benefits, provider networks, and the set of incentives their providers face (Clemens and Gottlieb (2017)). Hence, the treatment we study is a combination of the effect of Medicare for those who were previously uninsured and those with other forms of coverage at age 64.

similar.[3] The difference in the forecasts arises primarily due to large differences in the forecast reductions in collections balances *per newly-insured* individual in the two locations. In Raleigh, NC, the forecast reduction in collection balances was 956 dollars per newly-insured individual, 785% higher than the analogous forecast in San Francisco, CA.

Lastly, we examine how CZ-level forecasts changed due to the passage of the Affordable Care Act (ACA) in 2010, federal health reform legislation that substantially expanded coverage (e.g., Frean, Gruber and Sommers, 2017). Forecasts of the causal effect of expanding coverage on collections are smaller after the ACA's implementation in 2014 and have become more geographically concentrated in the South. This is because forecasted effects decreased by only 30% in the South (states like Mississippi, Texas, and Georgia) after the ACA's implementation, while they decreased by 50% in the rest of the country. Using a Kitagawa-Oaxaca-Blinder style decomposition, we show that this was due to the uniformity of ACA coverage gains across regions for the near-elderly—despite higher rates of uninsurance in the South—and, within the South, the fact that near-elderly uninsurance rates remain highest in areas where the financial health gains of expanding coverage per newly-insured are largest. These findings highlight a potential limitation of policies, such as the ACA, that delegate states considerable latitude in policy implementation, and a relative advantage of programs, such as Medicare, that are federally-administered—specifically, that the former may exacerbate geographic disparities while the latter tend to reduce them.

This paper makes three primary contributions. First, we contribute to a small existing literature that examines the financial risk protection provided by Medicare to elderly Americans (Finkelstein and McKnight, 2008; Engelhardt and Gruber, 2011; Barcellos and Jacobson, 2015; Dobkin et al., 2018; Caswell and Goddeeris, 2019; Batty, Gibbs and Ippolito, 2020) and a broader literature on the risk protection provided by health insurance (e.g., Gross and Notowidigdo, 2011; Finkelstein et al., 2012; Mazumder and Miller, 2016; Brevoort, Grodzicki and Hackmann, 2020; Hu et al., 2018) and the economic consequences of health shocks (e.g., Cochrane, 1991; Charles, 2003; Poterba, Venti and Wise, 2017; Dobkin et al., 2018; Meyer and Mok, 2019). We contribute to this literature in two ways. First, we examine the effect of Medicare at age 65 on a broad set of financial health outcomes from administrative credit report data. These results expand the outcomes of

[3] The near-elderly uninsurance rates in Raleigh, NC and San Francisco, CA during the period 2014-2017 were 6.5 and 5.9 percent, respectively.

Caswell and Goddeeris (2019) beyond just debt collections, and highlight that the financial health benefits of Medicare are concentrated in debt collections, with limited effects for other consumer credit outcomes. Second, we exploit our location-specific estimates of Medicare's causal effect to explore the effects of Medicare on the extensive margin (i.e., changes in insurance rates) and intensive margin (i.e., changes in financial health per newly-insured individual), and document considerable heterogeneity across geography in both.

Second, our work contributes to a growing literature on the geography of health and economic opportunity. Prior work has documented the important role that geography plays in economic opportunity (Chetty et al., 2014), healthcare utilization and spending (Finkelstein, Gentzkow and Williams, 2016; Cooper et al., 2018), and mortality (Finkelstein, Gentzkow and Williams, 2019). Recent work has also documented geographic concentration in financial strain (Keys, Mahoney and Yang, 2020), but causal evidence on the effects of geography on consumer financial strain is limited (Miller and Soo, 2018; Keys, Mahoney and Yang, 2020). We contribute a set of methods for estimating location-specific effects of Medicare and the extent to which they reduce geographic variation in financial health outcomes. Our findings suggest that differential access to health insurance is a key driver of the geographic variation in collections debt for the near-elderly, but less important in explaining differences across areas in other financial health outcomes.

Third, we use our locality-level estimates to investigate the incidence of Medicare. At $750 billion in annual spending (and growing), Medicare's incidence as one of the largest public programs is of first-order policy importance (McClellan and Skinner, 2006; Bhattacharya and Lakdawalla, 2006). We show that the gains in financial health due to Medicare are greatest in the South (and particularly the Deep South) where, in addition to there being a greater number of the uninsured, the financial health improvements per newly-insured person are the greatest.

2 Study data

In this section we briefly describe the data we use to construct area-level financial, demographic, health insurance, and healthcare market characteristics. Appendix A provides additional detail.

2.1 Financial outcomes data

The main dataset used in our analysis is the Federal Reserve Bank of New York's Equifax Consumer Credit Panel (CCP). The CCP is a five percent random sample of all individuals in the U.S. with credit reports.[4] The data include a comprehensive set of consumer credit outcomes quarterly from 1999 to 2017, including credit scores (originating from Equifax Risk Score 3.0), unsecured credit lines, auto loans, and mortgages. The data also include year of birth and zip code. No other demographic information is available. A major virtue of the CCP is its large sample size, which allows us to estimate the effect of Medicare separately for all 50 states and 741 commuting zones in the country. Our datasets include ages 55-64 ("the near-elderly") and 65-75 ("the elderly").

2.2 Demographic and health insurance data

For demographic and health insurance information, we draw on the American Community Survey (Ruggles et al., 2019). All analyses use samples constructed from the Public Use Microdata Area (PUMA) and state datasets, linked to the CZ- and state-level.[5] Demographic and health insurance variables from the ACS allow us to test for covariate smoothness to validate our RD design and examine the correlates of geographic heterogeneity in our treatment effects.

2.3 Additional area-level characteristics data

We constructed additional characteristics at the PUMA-level using data from the Healthcare Cost Report Information System (HCRIS) and the Dartmouth Atlas. From the HCRIS data, we construct PUMA-level measures of the share of hospital patient days at for-profit hospitals, teaching hospitals, and public hospitals in addition to other healthcare market characteristics. From the Dartmouth Atlas data, we measure the PUMA-level risk-adjusted Medicare spending per enrollee (Dartmouth Institute, 2019).

3 Empirical strategy: Regression discontinuity design

3.1 Econometric model

To estimate the causal impact of Medicare, we use an RD design that takes advantage of the sharp change in eligibility at age 65. We compare individuals just above and below the age 65 eligi-

[4] Lee and Van der Klaauw (2010) show that the CCP is reasonably representative of the U.S. population.
[5] Our cross-walk from PUMA to CZ uses David Dorn's crosswalks: https://www.ddorn.net/data.htm.

bility threshold under the assumption that individuals around the discontinuity are similar on observable and unobservable characteristics. Under this assumption, any discontinuities in financial health around age 65 can be attributed to the change in coverage as individuals age onto Medicare.

We estimate our regression discontinuity analyses both at the national level, and separately for each state and commuting zone,[6] using equations of the following form:

$$y_{i,l,t}(\text{age}) = \gamma \times 1(\text{age} > 65) + f\,(\text{age}) \times 1(\text{age} \leq 65) + g\,(\text{age}) \times 1(\text{age} > 65) + \epsilon_{i,l,t}(\text{age}). \quad (1)$$

where $y_{i,l,t}(\text{age})$ is an outcome for individuals i in location l in time period t of a given age. The functions $f\,(\text{age})$ and $g\,(\text{age})$ are the age profile of $y_{i,l,t}$ for those below the age of 65 and those above the age of 65, respectively, and control for the direct effect of age on outcomes. We denote the national-level effect of Medicare at age 65 as γ. We denote a set of γ_l, one for each location (either state or commuting zone) in our sample, as the location-level effect of Medicare at age 65, where $f(age)$ and $g(age)$ are allowed to vary by location.

The estimation of Equation 1 is complicated by two features of our data; First, our running variable, age, is measured discretely by year in our sample; Second, because we only observe birth year in the CCP data, and the data is quarterly, we measure age with noise. As a result, both the estimation and inference of $f(\cdot)$, $g(\cdot)$, and γ are more challenging, as error in measuring age 65 forces us to omit age 65 in our estimation procedure and use a "donut" RD, and the discreteness of the age variable requires further extrapolation.[7] To account for both issues, we follow the "honest" confidence intervals approach outlined in Kolesár and Rothe (2018), and Armstrong and Kolesár (2018*b*,*a*). Briefly, this approach bounds the second derivative of the true $f(\cdot)$ and $g(\cdot)$ functions near age 65, and uses this bound to estimate the maximum potential bias due to extrapolation. In our estimation, we report our point estimate and bias-adjusted 95% confidence intervals. See Appendix B for additional details.

Like all RD approaches, our design allows us to easily visualize the treatment effect γ using graphical methods. However, more uniquely in our setting, we also use our estimates to con-

[6] Commuting zones are groups of counties representing local labor markets (David and Dorn, 2013; Dorn, Hanson et al., 2019)

[7] The donut RD is a common solution to this problem in the literature (e.g., Barreca et al., 2011).

sider how Medicare changes the cross-location distribution of counterfactual outcomes at age 65. Denote the average counterfactual at age 65 for location l as $y_l(65-)$ and $y_l(65+)$, and define the causal effect of Medicare on the variance of outcomes across locations as $\phi = \frac{Var(y_l(65-))-Var(y_l(65+))}{Var(y_l(65-))}$, where the variance is taken across locations. This measure captures the change in geographic *variance* of our outcomes due to Medicare, rather than just the average level. We estimate standard errors and bias-adjusted confidence intervals for ϕ using the delta method following Armstrong and Kolesár (2018*a*), and report an estimated drop in variance for each of our outcomes along with bias-adjusted 95% confidence intervals. See Appendix B for additional details.

3.2 Forecasting the causal effects of Medicare by location

This section describes our approach to measuring the area-level factors associated with reductions in consumer financial strain at age 65 and constructing forecasts of the causal effects of Medicare by location.

We begin by estimating bivariate regressions between our locality-level causal effects of Medicare and location characteristics:

$$\hat{\gamma}_l = \alpha + X_l\omega + v_l. \tag{2}$$

where X_l is a scalar containing a single area-level characteristic (e.g. the share of black residents) and $\hat{\gamma}_l$ is our RD estimate for location l. We separately estimate ω for each characteristic, weighting the regression by each location's near-elderly population.

Given that many of the area-level characteristics we study are highly correlated, we re-estimate Equation 2 with the full set of area-level covariates:

$$\hat{\gamma}_l = \alpha + \vec{X}_l\vec{\omega} + v_l. \tag{3}$$

where $\vec{X}_l$ is the full set of area-level covariates. We estimate Equation 3 in two ways. First, we estimate the model using ordinary least squares (OLS) to recover the marginal association of each area-level characteristic with our locality-level causal estimates. Second, since the dimension of X_l is large (and many of the covariates are highly correlated), we use Lasso to perform covariate selection on $\vec{X}_l$, and then re-estimate the model using OLS (Belloni and Chernozhukov, 2013). This Lasso procedure lets us trade off between including multiple characteristics and constructing

predictions of $\hat{\gamma}_l$ with lower mean squared error.

We next construct forecasts of the causal effect of expanding Medicare (i.e., a reduction in the Medicare eligibility age) in each commuting zone. While our RD estimates of γ_l are unbiased forecasts, many are estimated with substantial estimation error. To reduce noise, we build on Chetty and Hendren (2018) and construct forecasts using a shrinkage estimator that combines our unbiased RD estimates and a predicted effect for each commuting zone using the covariates selected from our Lasso procedure (see Appendix B for additional details).

We repeat our approach for a scaled estimate $\beta_l = \gamma_l / \gamma_l^h$, where γ_l is a location-specific estimate of the effects of Medicare on financial health outcomes and γ_l^h is a location-specific estimate of the effects of Medicare on the insurance rate. This provides a measure of the effect of Medicare on financial health outcomes *per newly-insured individual* at each location. This helps account for the mechanical effect that areas with high near-elderly uninsurance rates will likely see large changes in financial health alongside increases in coverage. However, while we estimate β_l using fuzzy RD, it does *not* estimate the causal effect of insurance on financial health, as the characteristics of health insurance coverage also change for the previously-insured as they enter Medicare (Card, Dobkin and Maestas, 2008).

4 Results

4.1 Medicare, health insurance, and financial health, nationally and across states

Figure 1 presents the effect of Medicare at age 65 at the national level and for each state. In solid red circles, we plot the average national outcome for each age. At age 65, we plot two points: in the solid red triangle, we plot $y(65-)$, the national average at age 65 without Medicare and in the hollow red triangle we plot $y(65+)$, the national average at age 65 with Medicare. In gray, we repeat the same exercise for each of the states in our sample. For each outcome, we report the estimated national effect (with the bias-adjusted 95% confidence interval) and the estimated percent reduction in variance across states (with the bias-adjusted 95% confidence interval).

We plot the share of the population with health insurance coverage in Panel A of Figure 1. As has been documented previously (e.g., Card, Dobkin and Maestas, 2008), the effect of Medicare eligibility on the share of individuals with any form of coverage at age 65 is large—rising by 7.9

Figure 1: Changes in health insurance, financial health, and covariates at age 65

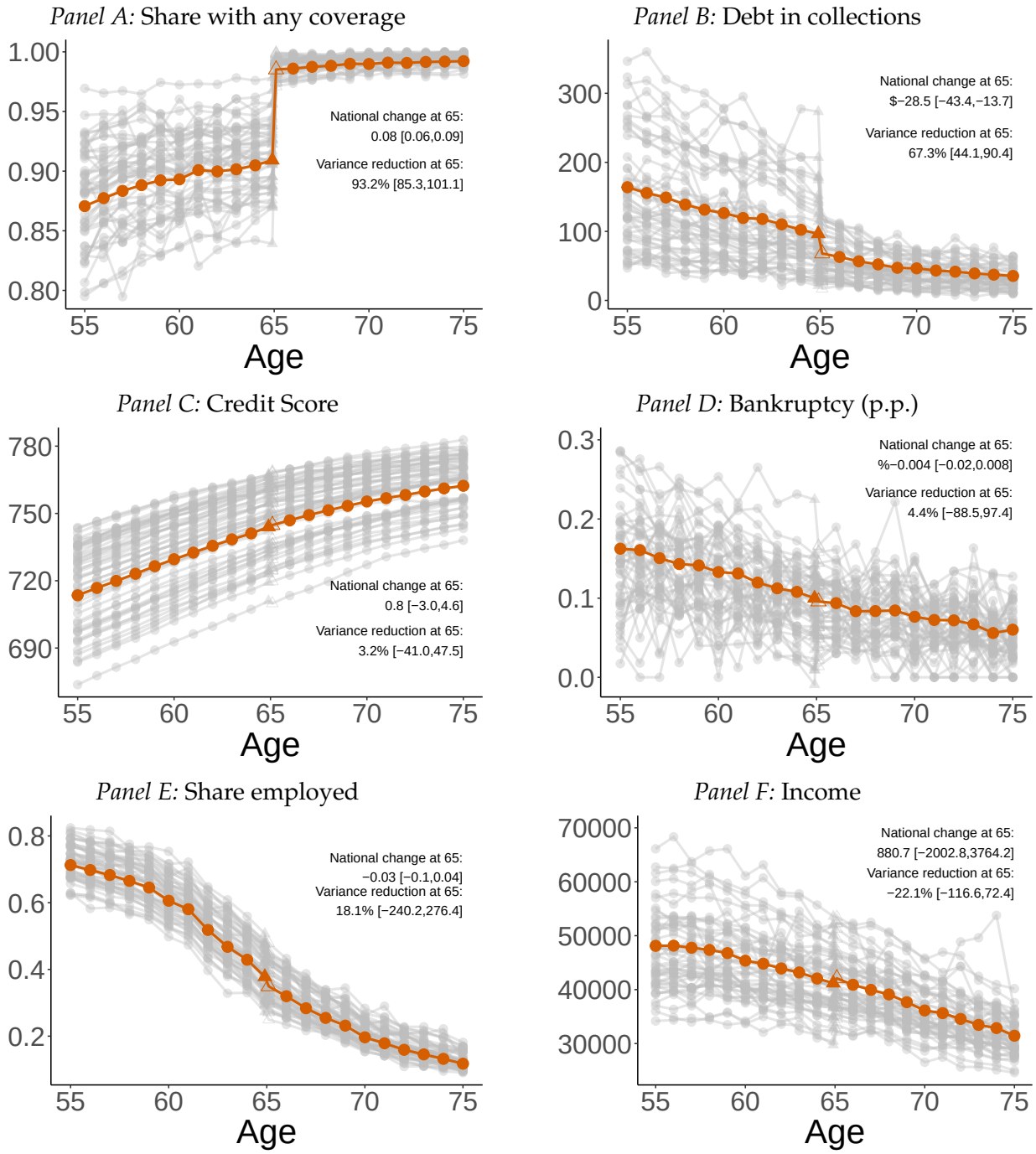

Note: This figure plots the average outcomes by age at both the national level (in red) and across the fifty U.S. states (in grey). The horizontal axis denotes age in years. The points plotted as circles reflect empirical averages from the data, while the triangles reflect imputed counterfactual values at age 65 from a local linear regression from the left and right (following Kolesár and Rothe (2018) and Armstrong and Kolesár (2018*a*)) with a bandwidth of 5. The imputed value without Medicare at age 65 is plotted at age 64.9, while the imputed value with Medicare at age 65 is plotted at age 65.1. Panel A plots the share of individuals with any form of health insurance. Panel B plots the average debts in collections over the past 12 months. Panel C plots the average Equifax Risk Score 3.0. Panel D plots the share of individuals with new bankruptcies (p.p.). Panel E plots the share of individuals employed. Panel F plots the average total income. The sample includes individuals who were age 55-75 between 2008 and 2017. See Section 2 for additional details on the outcomes and sample. Source: American Community Survey, 2008-2017 and New York Fed Consumer Credit Panel/Equifax, 2008-2017.

percentage points, relative to an overall insurance rate of almost 91 percent prior to Medicare. We estimate a sharp reduction in geographical variation in health insurance rates of 93.2% (95% CI: 85.3 to 101.1) at age 65 due to Medicare eligibility.[8] This suggests that Medicare, as expected, eliminates almost all variation across states in health insurance rates.

In Panel B of Figure 1, we also estimate a large national reduction in collections debt at age 65, with a sharp drop of 28.5 dollars (95% CI: -48.3 to -13.7).[9] We also estimate a corresponding reduction of 67.3% (95% CI: 44.1%-90.4%) in the overall cross-state variance of collections debt at age 65, consistent with the drop in variance for health insurance, implying that Medicare reduced the differences in collections debt across states by two-thirds.

In contrast, for our other financial health measures, we find statistically insignificant effects on credit score (Panel C) and bankruptcy (Panel D). The estimated variance reduction and national effects are small with large confidence bounds, suggesting that Medicare had limited effects on cross-state variance, despite large baseline differences across states. We also examine a variety of other financial health outcomes, including delinquent debt and foreclosure, and find small, though noisy, effects, with no corresponding reduction in national variance (Figure A2). In Appendix B we demonstrate that these results (and lack thereof) are robust to alternative specifications (Figures A3, A4, A5, A6, and Table A1).

In Panels E and F of Figure 1, we test our key identifying assumption that non-Medicare characteristics that affect outcomes do not jump discontinuously at age 65. For example, given that many individuals tend to retire in their early to mid-60s, we test whether this coincides with the age of eligibility for Medicare. We do not find evidence of discontinuities in non-Medicare characteristics at the national or local level at age 65. For both figures, we cannot reject the null that the effect size is zero at the national level, and that there is no change in the variance across states.

In Appendix B we examine potential discontinuities in additional covariates and present our estimates from state- and CZ-level covariate smoothness tests (Figures A7, A8, and A9). We find little evidence of discontinuities in the average values of covariates at age 65. Intuitively, while the

[8] Due to the asymptotic nature of these confidence intervals, the 95% CI includes values larger than the maximum possible value, 100%.

[9] We find a decline in especially large collections balances (Figure A1), consistent with evidence that Medicare curbs the upper tail of medical spending (Finkelstein and McKnight, 2008; Caswell and Goddeeris, 2019).

early to mid-60s are a time of transition for many individuals, the precise age of 65 is no longer a focal point for retirement decisions, which smooths out the timing of other lifestyle changes in a way that does not confound them with Medicare eligibility.

4.2 Medicare and the geography of financial strain

In this section, we seek to understand why the effect of Medicare on collections debt, where we find a large reduction in geographic variation, varies so much across localities.

Prior to individuals gaining Medicare eligibility at age 65, we observe large differences in collections debt across areas, with particularly high levels in the South. This feature of the US landscape of financial health is apparent in Figure 2, where we map the commuting zone estimates of counterfactual collections debt flows at age 65, with and without Medicare.[10] It is clear from Panel A that, absent Medicare, collections debt for the near-elderly varies widely across the country, with low levels in the Midwest and Northeast, and with high levels of debt collection concentrated in the South. At age 65, we observe a large reduction in collections, concentrated in the South. Panel B shows that much of the geographic variation in collections debt disappears at age 65, with lower (though still elevated) levels of collections debt in states like Mississippi, Texas, and Nevada.[11]

Why are collections so concentrated before Medicare and much less so after? One clear candidate is geographic differences in the uninsurance rate for the near-elderly. Prior work documents a link between health insurance coverage and collections debt (see e.g., Finkelstein et al., 2012), and we find similar associations between area-level health insurance rates and financial health outcomes among the near-elderly (Figure A10). We compare the estimated increase in health insurance due to Medicare to the drop in debt collections at the state-level and CZ-level in Figure A11. This "extensive margin" effect of Medicare on coverage explains a surprisingly large share of the variation (R^2 = 0.38), with small estimated reductions in collections for states with small estimated changes in the insurance rate at age 65.

These facts suggest that the effect of Medicare eligibility on debt collections may be driven by individuals who gain coverage, rather than those whose primary source of coverage is changing.

[10] For this map, due to smaller sample sizes, we use an empirical Bayes approach to shrink each locality-level estimate towards the overall average of the effects (see Appendix B).

[11] At the CZ-level, this reduction equates to a drop in the across-CZ variance in collections debt of 70% (very similar to our state-level estimate of 67.3%).

Figure 2: Counterfactual levels of collections debt by commuting zone at age 65 with and without Medicare

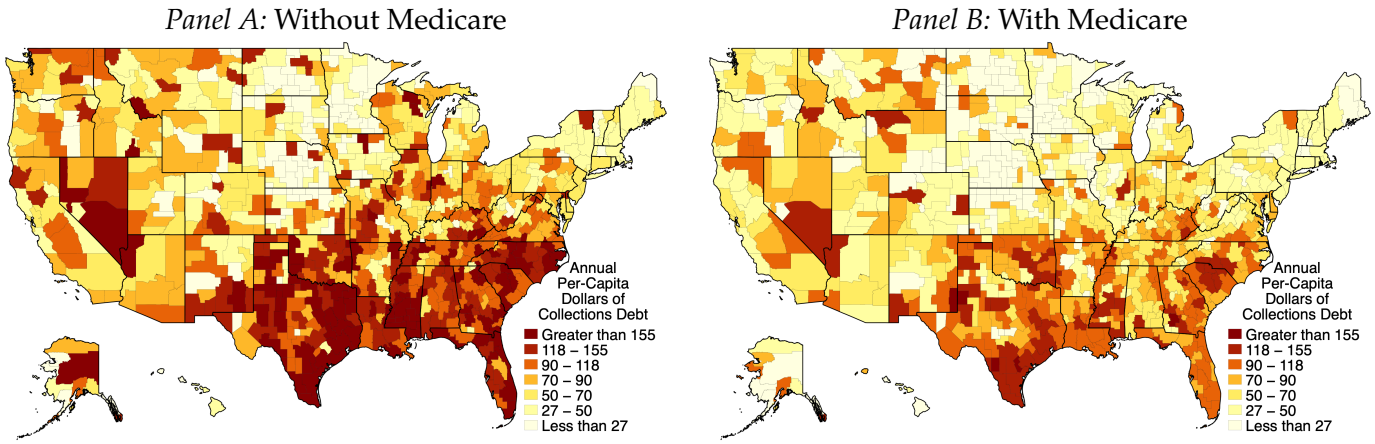

Note: This figure plots our counterfactual estimates of the flow of newly reported collections debt (within the past year) per capita at age 65, with and without Medicare. The CZ-level variance reduction at age 65—the difference in CZ-level variance between the two panels—was 63.8% (95% CI: 30.7%-97.0%). The counterfactuals are based on local linear regressions, done separately by commuting zone, using the methods from Kolesár and Rothe (2018). These estimates are then shrunk using empirical Bayes, described in Appendix B. Darker regions correspond to higher counterfactual collections debt per capita. Source: Consumer credit outcomes are based on 137,340,577 person-year observations from the New York Fed Consumer Credit Panel/Equifax, 2008-2017.

Motivated by this finding, we construct a scaled version of our CZ-level estimates, β_l, that measures the reduction in collections debt *per newly-insured*, and examine it alongside our *per capita* estimates going forward. This allows us to compare how the effects of Medicare differ across locations with different baseline levels of uninsurance among the near-elderly.

We now examine what other area-level factors are associated with the reductions in collections debt at age 65. We present evidence that commuting zones with larger shares of black residents, people with disabilities, and for-profit hospitals experience the largest gains in financial health at age 65, across a variety of estimation approaches.

Figure 3 presents correlations between our area-level characteristics and estimated effects of Medicare. The leftmost panel presents the coefficients from separate bivariate OLS regressions of our regression discontinuity estimates of CZ-level reductions in collections debt *per capita* (in red circles) and *per newly-insured* (in blue triangles) on CZ-level demographic and healthcare market characteristics, with bars representing the 95% confidence intervals. Since many of the area-level characteristics are highly correlated, the center and right panels plot multivariate and post-Lasso analyses describing the partial correlations between the characteristics and our locality-

Figure 3: Commuting zone characteristics correlated with the reduction in collections debt at age 65

Panel A: Demographic characteristics

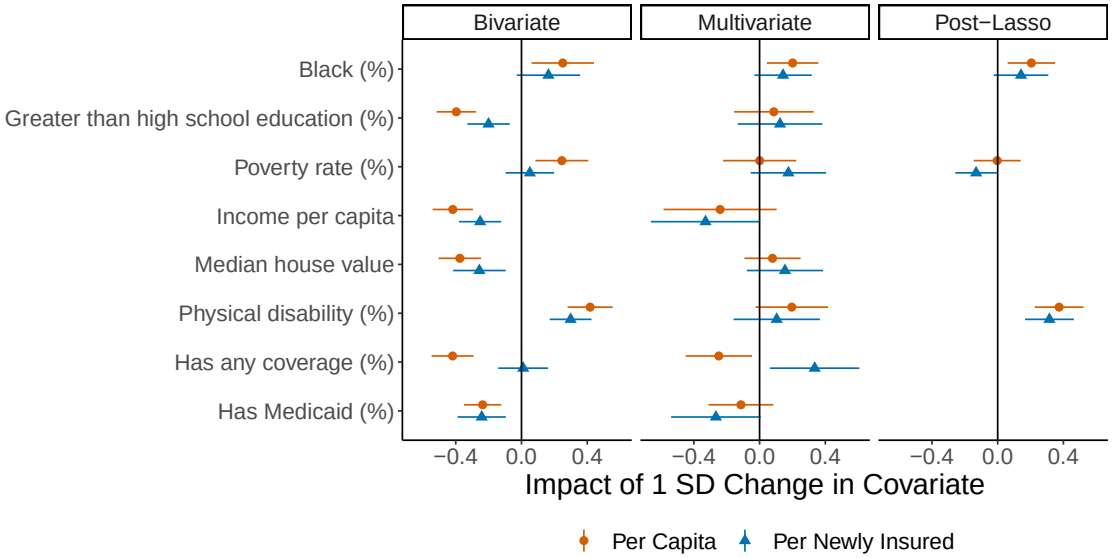

Panel B: Healthcare market characteristics

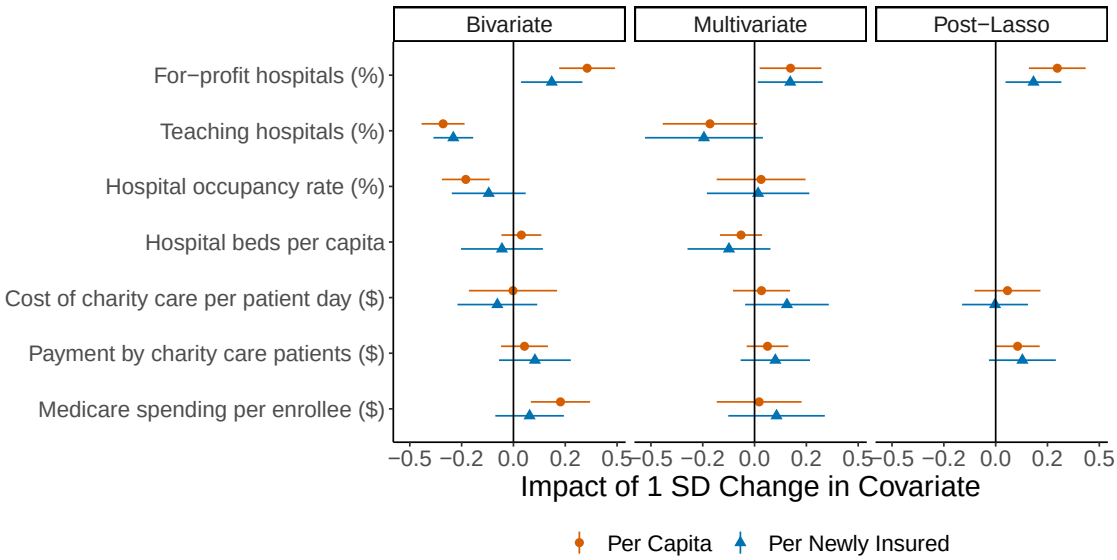

Note: This figure plots bivariate OLS estimates (left panel), multivariate OLS estimates (center panel), and post-Lasso multivariate estimates (right panel) of CZ-level estimated reductions in collections debt per capita on a set of CZ-level characteristics. We standardize all the variables so the coefficients reflect the strength of the association between a one standard deviation change in the covariate and the estimated reduction in collections debt at age 65. The horizontal bars are 95% confidence intervals. The multivariate OLS regression results and post-Lasso multivariate regression results are both run on the full set of characteristics in Panels A and B. For post-Lasso, we first estimate a Lasso regression on the full set of characteristics and then report the results of multivariate OLS run on the characteristics chosen by the Lasso regression. Tabular versions of these results are in Table A4. Source: Consumer credit outcomes are based on 137,340,577 person-year observations from the New York Fed Consumer Credit Panel/Equifax, 2008-2017. CZ-level uninsurance rates are from the American Community Survey, 2008-2017. Healthcare market characteristics are from the Healthcare Cost Report Information System (HCRIS) and the Dartmouth Atlas. For additional details on the data see Section 2.

level causal estimates. We separate the demographic and healthcare market characteristics into two panels for presentation purposes, but all covariates are jointly combined in estimation for the multivariate and post-Lasso models. To facilitate comparison across the area-level correlates and the *per capita* and *per newly-insured* measures, we standardize all the area-level correlates, and then divide the coefficients by the respective national *per capita* or *per newly-insured* estimates. Hence, plotted coefficients in Figure 3 correspond to the effect of a one standard deviation change in the covariate on a percentage change in the reduction in debt collections at age 65. Hence, a coefficient of 0.1 implies a 10% increase in the effect of Medicare in reducing debt collections from a one standard deviation change in the covariate.

Panel A of Figure 3 shows that the share of high school graduates, income per capita, and median house values in a CZ were all associated with smaller reductions in *per capita* collections debt at age 65. Unsurprisingly, the share of residents with health insurance (or Medicaid), was also associated with a smaller reduction in per capita collections debt at age 65. The share of black residents, the poverty rate, and the share of people with disabilities, on the other hand, were associated with larger reductions in collections at age 65. In multivariate and post-Lasso analyses, only the near-elderly health insurance rate and the high school graduation rate were associated with smaller reductions in per capita collections, while the share of black residents and people with disabilities in a CZ were consistently associated with larger reductions in per capita collections.[12] Including Census region or division fixed effects—and using only the within-area, across-CZ variation that remains—does not qualitatively change our results (Figure A12). Once we restrict to only using variation across CZs, but within states, however, the association between the share of black residents and per capita reductions in collections is severely attenuated.

Panel B of Figure 3 presents the healthcare market characteristics correlated with our estimates. In the bivariate OLS model, a higher share of for-profit hospitals and higher risk-adjusted spending per Medicare beneficiary were both associated with larger reductions in collections debt at age 65, while a higher share of teaching hospitals and higher hospital occupancy rates were associated with smaller reductions in collections at age 65. In multivariate OLS and post-Lasso analyses, only the CZ-level share of for-profit hospitals was associated with our causal CZ-level

[12]While the Lasso procedure did not select the near-elderly health insurance rate, we note a very high correlation between that measure and the high school graduation rate ($\rho = 0.45$).

effects, with a one standard deviation increase in the share of for-profit hospitals associated with a 40% larger reduction in *per capita* collections at 65. Unlike not-for-profit hospitals, for-profits are not required to provide charity (discounted or free) care and evidence suggests that they offer less charity care than not-for-profit hospitals (e.g., Horwitz, 2005; Schlesinger and Gray, 2006; Valdovinos, Le and Hsia, 2015).[13] Figure A12 demonstrates that the relationship between for-profit hospital share and CZ-level reductions in per capita collections debt at age 65 is robust to the inclusion of fixed effects for census regions or divisions, but not states.

Figure 3 also examines the demographic and healthcare market characteristics associated with reductions in collections debt *per newly-insured*. This exercise accounts for the change in the uninsurance rate at age 65, to identify CZs that experienced larger or smaller reductions in debt collections not mechanically driven by Medicare's "extensive margin" effect on coverage. The share of people with disabilities and for-profit hospitals in a CZ is consistently associated with larger reductions in collections debt per newly-insured. In addition, CZs with a larger share of black residents—where we see large reductions in *per capita* collections debt—also appear to experience larger reductions in collections *per newly-insured*. The other area-level characteristics were not consistently associated with the estimated reductions in collections debt per newly-insured.

4.3 Forecasts of the causal effects of Medicare on financial strain

Given that the effect of Medicare varies substantially across localities, where would the effects of a broad expansion of coverage to the near-elderly (i.e., by lowering the Medicare eligibility age) be the largest? In what follows, we discuss our forecasts of CZ-level causal effects, how those forecasts have changed post-ACA, and their implications for future potential coverage expansions.

In Panel A of Figure 4, we map the *per capita* mean-square error minimizing forecast causal effects, $\hat{\gamma}_l^f$, across CZs for the near-elderly, with darker colors depicting areas predicted to experience larger reductions in collections-related strain associated with an expansion of (nearly) universal health insurance to the near-elderly. The largest forecast reductions are concentrated in the South, ranging from \$20-\$50 in most CZs. The opposite is true in the Midwest, where forecast reductions in consumer financial strain are small across all CZs.[14] In Panel B, we map the

[13] In addition, hospitals in markets with a higher share of for-profits respond to competition by reducing charity care and trying to avoid the uninsured (Frank, Salkever and Mitchell, 1990).

[14] Table A2 lists the forecasts for the 50 commuting zones with the largest near-elderly populations (accounting for 53.2% of the near-elderly US population during our sample period).

Figure 4: Forecasts of causal reductions in collections debt from expanding health insurance to the near-elderly by commuting zone

Panel A: Per capita, 2008-2017

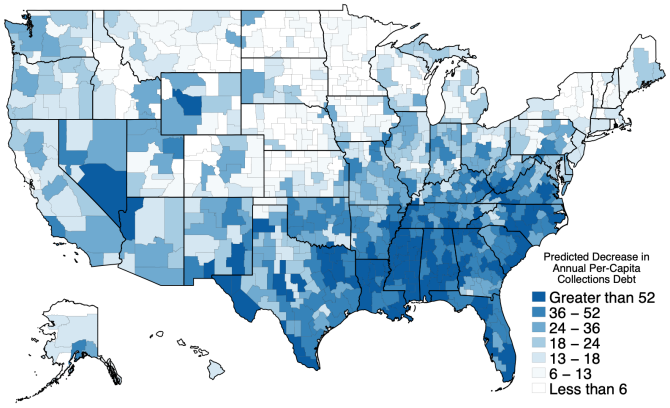

Panel B: Per newly insured, 2008-2017

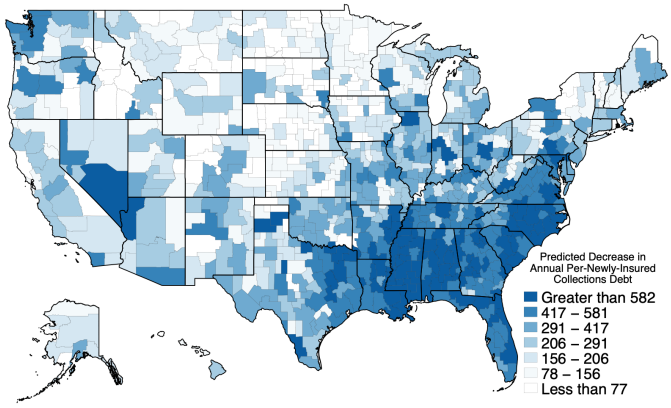

Note: This figure plots mean square error (MSE)-minimizing forecasts of the reductions in collections debt per capita (Panel A) and the reduction in collections debt per newly-insured (Panel B). We construct the MSE-minimizing forecasting by first running a Lasso regression to predict the CZ-level reductions in collections debt per capita (or per newly-insured) as discussed in Section 3. This generates a prediction for each CZ, which we call $\hat{\gamma}_l$. Following Chetty and Hendren (2018) we then combine the $\hat{\gamma}_l$ estimates with our estimates of γ_l to construct the MSE-minimizing forecast for each commuting zone, γ_l^f. Source: Consumer credit outcomes are based on 137,340,577 person-year observations from the New York Fed Consumer Credit Panel/Equifax, 2008-2017. CZ-level uninsurance rates are from the American Community Survey, 2008-2017. Healthcare market characteristics are from the Healthcare Cost Report Information System (HCRIS) and the Dartmouth Atlas. For additional details on the data see Section 2.

forecasts per newly-insured at age 65, $\hat{\beta}_l^f$. Despite large geographic differences in the near-elderly uninsurance rate, the maps are strikingly similar, with the largest forecast reductions in collections debt per newly-insured also concentrated in the South. This is consistent with the Lasso procedure selecting similar area-level characteristics when predicting changes in per capita and per newly-insured debt collections at age 65.[15]

We next examine how these forecasts have changed due to the ACA, federal health reform legislation that substantially expanded coverage (Frean, Gruber and Sommers, 2017). Panel A of Figure 5 presents the forecasts using the sample before and after the implementation of the ACA. On the x-axis, we plot the pre-ACA per capita forecast reductions in collections, and on the y-axis, the post-ACA per capita forecast reductions. The forecast reductions post-ACA are generally smaller than pre-ACA, which results in the majority of commuting zones below the 45-degree line. Rather than having a uniform effect across CZs on collections forecasts, which would appear as a vertical shift in the cloud of points, the ACA led to a "rotation" in the forecasts; CZs with larger

[15]We plot the relationship between the two forecasts across CZs in Figure A13 and find an R^2 of 0.8213.

Figure 5: Forecasts of causal reductions in collections debt at the commuting zone level before and after the Affordable Care Act (ACA)

Panel A: Pre and Post-ACA Per Capita Forecasts

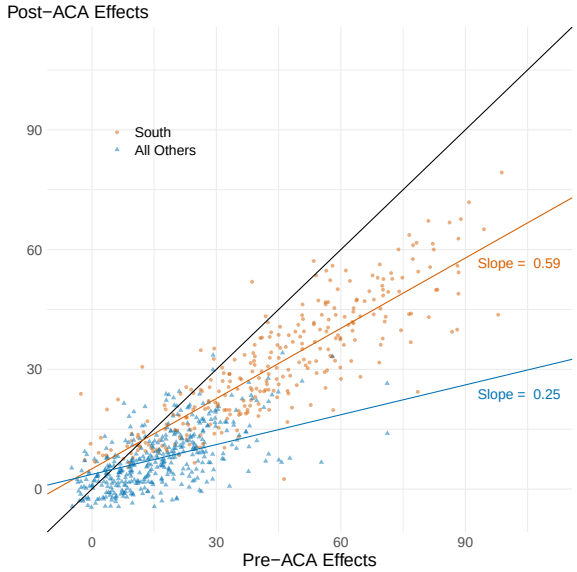

Panel B: Decomposing Changes in Forecasts

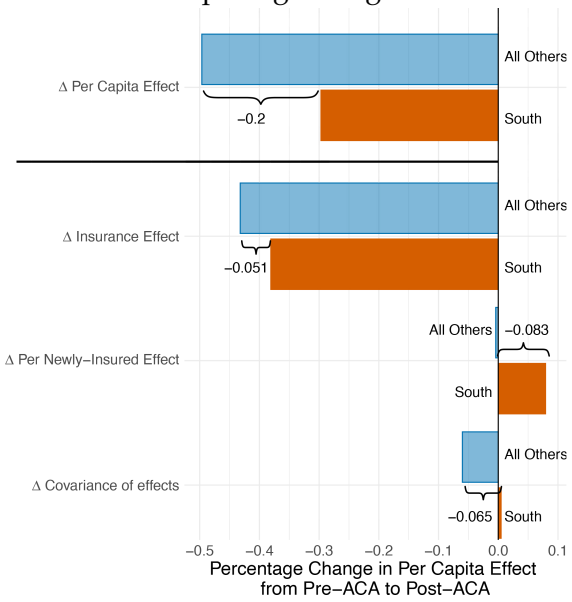

Note: Panel A of this figure plots mean square error (MSE)-minimizing forecasts of the CZ-level reductions in collections debt per capita in the pre-ACA period on the x-axis against the analogous post-ACA period forecast on the y-axis. We separately plot commuting zones in the South in orange circles and all other commuting zones with blue triangles. Fitted lines are constructed using bivariate OLS. We construct the MSE-minimizing forecasting by first running a Lasso regression to predict the CZ-level reductions in collections debt per capita separate for each period as discussed in Section 3. This generates a prediction for each CZ in each period, which we call $\hat{\gamma}_l$. Following Chetty and Hendren (2018) we then combine the $\hat{\gamma}_l$ estimates with our estimates of γ_l to construct the mean square error-minimizing forecast for each commuting zone in each period, γ_l^f. Panel B of this figure plots the average percentage decline in per capita forecasted effects for the South and non-South regions, and the decomposition described in the text and Appendix B. The top bars present the average percentage decline in per capita forecasted effects for the South and non-South regions. The second set of bars present the decline due to the change in insurance coverage rates, holding fixed the per newly-insured effect. The third set of bars present the decline due to the change in the per newly-insured effect, holding fixed the impact on insurance coverage rates. The last set of bars is due to the change in covariance between the per newly-insured effect and the effect on insurance. In curly braces for each set of bars we report the difference between the non-South and South averages. Source: Consumer credit outcomes are based on 137,340,577 person-year observations from the New York Fed Consumer Credit Panel/Equifax, 2008-2017. CZ-level uninsurance rates are from the American Community Survey, 2008-2017. For additional details on the data see Section 2.

pre-ACA forecasts experienced larger changes in forecast pre- to post-ACA. This is consistent with the increase in health insurance coverage due to the ACA (Frean, Gruber and Sommers, 2017). However, the degree of rotation varied significantly by geography. The forecasts fell less in the South than elsewhere. As a result, the effect of Medicare on collections-related financial strain have become much more geographically-concentrated in the South, and particularly the "Deep South" region comprised of Louisiana, Alabama, Mississippi, Georgia, South Carolina, and parts of Texas and Florida (Figure A14).

Why did the forecast reductions in collections fall less in the South than elsewhere? Panel B of Figure 5 documents that average CZ-level forecasts decreased by only 30% in the South after

the ACA's implementation, but 50% elsewhere. We decompose the differential change in forecasts (i.e., the 30% vs. 50%) using a Kitagawa-Oaxaca-Blinder style decomposition (Kitagawa, 1955; Oaxaca, 1973; Blinder, 1973). Intuitively, this decomposes the change in the forecast reductions in collections debt per capita into changes in the extensive margin "any health insurance" effect, changes in the intensive margin "reduction in collections per newly-insured" effect, and a residual term that reflects the changing covariance between the two (see Appendix B for additional details). We find that the differential change in forecasts between regions was driven by all three pieces. First, uniform gains in ACA coverage across regions for the near-elderly (Figure A16)—despite higher pre-existing rates of uninsurance in the South—led to smaller reductions, percentage-wise, in uninsurance rates in the South as compared to elsewhere.[16] This accounted for one-quarter of the differential change in forecasts between regions (0.051/0.2). Second, the forecast reductions in collections debt per newly-insured *increased* in the South (where they were larger to begin with) after the ACA, but remained unchanged elsewhere (Figure A17). This accounted for two-fifths of the differential change in forecasts (0.083/0.2). Lastly, in the non-south CZs, the covariance between the per newly-insured effect and the effect on the share of individuals covered *decreased* post-ACA, whereas it was unchanged in the South. This suggests that the ACA expansions in the South were not as well targeted (on this dimension) as those elsewhere in the country. The poorer targeting explained the remaining third (0.065/0.2) of the differential change in forecasts between regions.

5 Conclusion

This paper examines the relationship between health insurance and financial health by studying financial outcomes for individuals as they age onto Medicare at 65. We find a 30 percent reduction in debt collections—and a two-thirds reduction in the geographic variation in collections—at age 65, with limited effects on other financial outcomes. Areas that experienced larger gains in financial health at age 65 had higher shares of black residents, people with disabilities, and for-profit hospitals.

Our data suggest that the financial health benefits of potential future coverage expansions to

[16] This left the uninsured near-elderly population more concentrated in the South after the implementation of the ACA (Figure A15).

the near-elderly have become more geographically concentrated in the South after the passage of the ACA. This is due to the uniform gains across regions in coverage for the near-elderly due to the ACA—despite higher pre-existing rates of uninsurance in the South—and, within the South, the fact that uninsurance rates remain high in areas where the financial health gains per newly-insured are largest. These findings highlight a potential limitation of policies, such as the ACA, that delegate states considerable latitude in policy implementation, and a relative advantage of programs, such as Medicare, that are federally-administered—specifically, that the former may exacerbate geographic disparities while the latter tend to reduce them.

References

Armstrong, Timothy, and Michal Kolesár. 2018*a*. "Simple and honest confidence intervals in nonparametric regression." Cowles Foundation Discussion Paper.

Armstrong, Timothy B, and Michal Kolesár. 2018*b*. "Optimal inference in a class of regression models." *Econometrica*, 86(2): 655–683.

Barcellos, Silvia Helena, and Mireille Jacobson. 2015. "The effects of Medicare on medical expenditure risk and financial strain." *American Economic Journal: Economic Policy*, 7(4): 41–70.

Barreca, Alan I, Melanie Guldi, Jason M Lindo, and Glen R Waddell. 2011. "Saving babies? Revisiting the effect of very low birth weight classification." *The Quarterly Journal of Economics*, 126(4): 2117–2123.

Batty, Michael, Christa Gibbs, and Benedic Ippolito. 2020. "Health insurance , medical debt , and financial." *AEI Economics Working Paper*, , (June).

Belloni, Alexandre, and Victor Chernozhukov. 2013. "Least squares after model selection in high-dimensional sparse models." *Bernoulli*, 19(2): 521–547.

Bhattacharya, Jay, and Darius Lakdawalla. 2006. "Does Medicare benefit the poor?" *Journal of Public Economics*, 90(1-2): 277–292.

Blinder, Alan S. 1973. "Wage discrimination: reduced form and structural estimates." *Journal of Human resources*, 436–455.

Brevoort, Kenneth, Daniel Grodzicki, and Martin B Hackmann. 2020. "The credit consequences of unpaid medical bills." *Journal of Public Economics*, 187: 104203.

Calonico, Sebastian, Matias D Cattaneo, and Rocio Titiunik. 2015. "rdrobust: An r package for robust nonparametric inference in regression-discontinuity designs." *R Journal*, 7(1): 38–51.

Card, David, Carlos Dobkin, and Nicole Maestas. 2008. "The impact of nearly universal insurance coverage on health care utilization: evidence from Medicare." *American Economic Review*, 98(5): 2242–58.

Caswell, Kyle J., and John H. Goddeeris. 2019. "Does Medicare Reduce Medical Debt?" *American Journal of Health Economics*, 0(ja): null.

Cattaneo, Matias D, Richard K Crump, Max H Farrell, and Yingjie Feng. 2019. "On binscatter." *arXiv preprint arXiv:1902.09608*.

Charles, Kerwin Kofi. 2003. "The longitudinal structure of earnings losses among work-limited disabled workers." *Journal of human Resources*, 38(3): 618–646.

Chetty, Raj, and Nathaniel Hendren. 2018. "The impacts of neighborhoods on intergenerational mobility II: County-level estimates." *The Quarterly Journal of Economics*, 133(3): 1163–1228.

Chetty, Raj, Nathaniel Hendren, Patrick Kline, and Emmanuel Saez. 2014. "Where is the land of opportunity? The geography of intergenerational mobility in the United States." *The Quarterly Journal of Economics*, 129(4): 1553–1623.

Clemens, Jeffrey, and Joshua D Gottlieb. 2017. "In the shadow of a giant: Medicare's influence on private physician payments." *Journal of Political Economy*, 125(1): 000–000.

Cochrane, John H. 1991. "A simple test of consumption insurance." *Journal of political economy*, 99(5): 957–976.

Cooper, Zack, Stuart V Craig, Martin Gaynor, and John Van Reenen. 2018. "The price ain't right? Hospital prices and health spending on the privately insured." *The Quarterly Journal of Economics*, 134(1): 51–107.

Dartmouth Institute. 2019. "Dartmouth Atlas of Health Care."

David, H, and David Dorn. 2013. "The growth of low-skill service jobs and the polarization of the US labor market." *American Economic Review*, 103(5): 1553–97.

Dobkin, Carlos, Amy Finkelstein, Raymond Kluender, and Matthew J Notowidigdo. 2018. "The economic consequences of hospital admissions." *American Economic Review*, 108(2): 308–52.

Dorn, David, Gordon Hanson, et al. 2019. "When Work Disappears: Manufacturing Decline and the Falling Marriage Market Value of Young Men." *American Economic Review: Insights*, 1(2): 161–78.

Duggan, Mark, Atul Gupta, and Emilie Jackson. 2019. "The Impact of the Affordable Care Act: Evidence from California's Hospital Sector." National Bureau of Economic Research.

Engelhardt, Gary V, and Jonathan Gruber. 2011. "Medicare Part D and the financial protection of the elderly." *American Economic Journal: Economic Policy*, 3(4): 77–102.

Finkelstein, Amy, and Robin McKnight. 2008. "What did Medicare do? The initial impact of Medicare on mortality and out of pocket medical spending." *Journal of public economics*, 92(7): 1644–1668.

Finkelstein, Amy, Matthew Gentzkow, and Heidi L Williams. 2019. "Place-based drivers of mortality: Evidence from migration." National Bureau of Economic Research.

Finkelstein, Amy, Matthew Gentzkow, and Heidi Williams. 2016. "Sources of geographic variation in health care: Evidence from patient migration." *The quarterly journal of economics*, 131(4): 1681–1726.

Finkelstein, Amy, Sarah Taubman, Bill Wright, Mira Bernstein, Jonathan Gruber, Joseph P Newhouse, Heidi Allen, Katherine Baicker, and Oregon Health Study Group. 2012. "The Oregon health insurance experiment: evidence from the first year." *The Quarterly journal of economics*, 127(3): 1057–1106.

Frandsen, Brigham R, Markus Frölich, and Blaise Melly. 2012. "Quantile treatment effects in the regression discontinuity design." *Journal of Econometrics*, 168(2): 382–395.

Frank, RG, DS Salkever, and J Mitchell. 1990. "Market forces and the public good: competition among hospitals and provision of indigent care." *Advances in health economics and health services research*, 11: 159.

Frean, Molly, Jonathan Gruber, and Benjamin D Sommers. 2017. "Premium subsidies, the mandate, and Medicaid expansion: Coverage effects of the Affordable Care Act." *Journal of Health Economics*, 53: 72–86.

Gross, Tal, and Matthew J Notowidigdo. 2011. "Health insurance and the consumer bankruptcy decision: Evidence from expansions of Medicaid." *Journal of Public Economics*, 95(7): 767–778.

Horwitz, Jill R. 2005. "Making profits and providing care: comparing nonprofit, for-profit, and government hospitals." *Health affairs*, 24(3): 790–801.

Hu, Luojia, Robert Kaestner, Bhashkar Mazumder, Sarah Miller, and Ashley Wong. 2018. "The effect of the affordable care act Medicaid expansions on financial wellbeing." *Journal of public economics*, 163: 99–112.

Imbens, Guido, and Stefan Wager. 2019. "Optimized regression discontinuity designs." *Review of Economics and Statistics*, 101(2): 264–278.

Keys, Benjamin J, Neale Mahoney, and Hanbin Yang. 2020. "What Determines Consumer Financial Distress? Place-and Person-Based Factors." National Bureau of Economic Research.

Kitagawa, Evelyn M. 1955. "Components of a difference between two rates." *Journal of the american statistical association*, 50(272): 1168–1194.

Kolesár, Michal, and Christoph Rothe. 2018. "Inference in regression discontinuity designs with a discrete running variable." *American Economic Review*, 108(8): 2277–2304.

Lee, David S, and David Card. 2008. "Regression discontinuity inference with specification error." *Journal of Econometrics*, 142(2): 655–674.

Lee, Donghoon, and Wilbert Van der Klaauw. 2010. "An introduction to the frbny consumer credit panel." FRB of New York Staff Report 479.

Mazumder, Bhashkar, and Sarah Miller. 2016. "The effects of the Massachusetts health reform on financial distress." *American Economic Journal: Economic Policy*, 8(3): 284–313.

McClellan, Mark, and Jonathan Skinner. 2006. "The incidence of Medicare." *Journal of Public Economics*, 90(1-2): 257–276.

Meyer, Bruce D, and Wallace KC Mok. 2019. "Disability, earnings, income and consumption." *Journal of Public Economics*, 171: 51–69.

Miller, Sarah, and Cindy K Soo. 2018. "Do Neighborhoods Affect Credit Market Decisions of Low-Income Borrowers? Evidence from the Moving to Opportunity Experiment." National Bureau of Economic Research.

Morris, Carl N. 1983. "Parametric empirical Bayes inference: theory and applications." *Journal of the American statistical Association*, 78(381): 47–55.

Oaxaca, Ronald. 1973. "Male-female wage differentials in urban labor markets." *International economic review*, 693–709.

Poterba, James M, Steven F Venti, and David A Wise. 2017. "The asset cost of poor health." *The Journal of the Economics of Ageing*, 9: 172–184.

Ruggles, Steven, Sarah Flood, Ronald Goeken, Josiah Grover, Erin Meyer, Jose Pacas, and Matthew Sobek. 2019. "IPUMS USA: Version 9.0 [dataset]."

Schlesinger, Mark, and Bradford H Gray. 2006. "How Nonprofits Matter In American Medicine, And What To Do About It: Reports of the demise of nonprofits in US health care are premature." *Health affairs*, 25(Suppl1): W287–W303.

Valdovinos, Erica, Sidney Le, and Renee Y Hsia. 2015. "In California, not-for-profit hospitals spent more operating expenses on charity care than for-profit hospitals spent." *Health Affairs*, 34(8): 1296–1303.

For Online Publication

Appendix for:

The Great Equalizer: Medicare and the Geography of Consumer Financial Strain

A Study data

A.1 Financial outcomes data

The main dataset used in our analysis is the Federal Reserve Bank of New York's Equifax Consumer Credit Panel (CCP). The CCP is a five percent random sample of all individuals in the U.S. with credit reports. The CCP data is a representative sample of all individuals with a credit report but it does not include the roughly 11 percent of the U.S. population without credit reports. As a result, the CCP data is more representative for high-income individuals than for low-income individuals, and it is more representative for older than younger people. Lee and Van der Klaauw (2010) show that the CCP is reasonably representative of the U.S. population with the possible exception of very young adults, suggesting that sample representativeness should not be a concern in our application.

The data include a comprehensive set of consumer credit outcomes from quarterly from the first quarter of 1999 to the fourth quarter of 2017, including information on credit scores (originating from Equifax Risk Score 3.0), unsecured credit lines, auto loans, and mortgages. The data also include year of birth and precise geographic location at the census block level. No other demographic information is available at the individual level.

A major virtue of the CCP is its large sample size, which allows us to measure financial outcomes at granular geographic levels with precision. This is key to our RD estimation strategy across geographies, where we estimate the effect of Medicare separately for 50 states and 741 commuting zones in the country. For our analyses, we aggregate the data to locality-by-age-by-year cells and weight by the underlying population in each cell. Since we only observe birth year, and the data is quarterly, age is measured with noise. For example, all individuals with birth year 1940 are measured as age 65 in the first quarter of 2005, while in reality some of these individuals will turn 65 later in the year. We address this using a "donut" RD procedure which we discuss in more detail in Section 3.

The financial health variables that we focus on from the CCP are the size of accounts sent to collection agencies (usually, these are accounts that have been delinquent for over 90 days), the size of accounts that are delinquent, the Equifax Risk Score, as well as additional financial health outcomes (e.g., bankruptcy). Refer to Appendix Table A3 for the definitions of each of the financial health outcomes we use from the CCP.

We examine the impact of Medicare on the distributions of three of our outcome measures: amount of debt in collections, total amount of debt in delinquency, and amount of credit card debt in delinquency. For all three of these cases, we would expect that large out-of-pocket expenses would cause increases in the right tail of the distribution. To examine this, we calculate the share of the population in a county-year-age bin that has amounts in the following bins: 1-500, 501-1,000, 1,001-2,500, 2,501-5,000, 5,001-10,000, and greater than 10,000 dollars. The residual category is any person with 0 dollars. We use the share within a given bin as the outcome variable in our main specification, so that our estimate is the change in the relative share of individuals within each bin due to Medicare eligibility.[1]

[1] An alternative approach would be to directly estimate quantile treatment effects using regression discontinuity,

A.2 Demographic and health insurance data

For demographic and health insurance information, we draw on the American Community Survey (Ruggles et al., 2019). All analyses use samples constructed from the PUMA and state datasets, linked to the Commuting Zone (CZ)- and state-level. Our cross-walk from PUMA to Commuting Zones uses David Dorn's crosswalks (available here: https://www.ddorn.net/data.htm).

Demographic data. We construct demographic variables from the ACS at the PUMA-by-age-by-year level and then crosswalk to the CZ- and state-level to test for covariate smoothness in validating our RD design and to examine the correlates of geographic heterogeneity in our treatment effects. From the ACS, we measure the homeownership rate, marital status, race, educational attainment, employment status, usual hours worked per week, total personal income, social security income, poverty status, and disability rate.

Health insurance data. The ACS also allows us to construct health insurance variables from the ACS at the PUMA-by-age-by-year level to test for changes in health insurance at age 65 and to examine the correlates of geographic heterogeneity in our treatment effects. From the ACS, we measure the share of individuals in each cell with any health insurance coverage.

A.3 Additional area-level characteristics data

In addition to the CCP and ACS data, we constructed additional characteristics at the PUMA-level. These characteristics are drawn from several places, including the Healthcare Cost Report Information System (HCRIS) and the Dartmouth Atlas. From the HCRIS data, we construct PUMA-level measures of the share of hospital patient days at for-profit hospitals, teaching hospitals, and public hospitals. We also measure the average hospital occupancy rate at the PUMA-level and the hospital beds per capita. In addition, for the period 2010-2017 we measure PUMA-level reported charity care costs per patient day and payments recovered by hospitals from charity care patients by patient day. From the Dartmouth Atlas data, we measure the PUMA-level risk-adjusted Medicare spending per enrollee (Dartmouth Institute, 2019).

B Additional Methods and Robustness

B.1 Honest RD and Shrinkage Estimators

Robustness using Honest RD As discussed in Section 3, we account for discreteness and measurement error in our running variable, age, by following the "honest" confidence intervals approach outlined in Kolesár and Rothe (2018), and Armstrong and Kolesár (2018*b*,*a*). This method requires an additional tuning parameter, K, which imposes an upper bound on the absolute value of the second derivative of the conditional expectation function. Intuitively, this method places a bound on how quickly the functions $f(\cdot)$ and $g(\cdot)$ can change. To choose our value of K for our main estimates, we follow an approach similar to the approach advocated in Imbens and Wager (2019). We take a large window to the left of the RD cutoff and fit a quadratic function of age to the data. We take the coefficient on the quadratic term (the second derivative), take the absolute value, and multiply it by four. We take this as our estimate of K. Similar to robustness exercises with bandwidths in previous RD methods, we present additional robustness tests which vary the value of K by changing the number that we scale this second derivative by in Appendix Figures A3 and A5.

such as those proposed in Frandsen, Frölich and Melly (2012). However, we are not able to easily account for the discrete running variable in our estimation process using quantile treatment effects. As a result, we focus on our share-based approach.

Inference for variance reduction Our estimate of cross-state and cross-CZ variance reduction due to the Medicare is a non-linear functional of the different estimates of a local non-parametric estimate. Specifically, we are interested in $T(f,g) = \phi(f,g)$, where

$$\phi(f,g) = 1 - \frac{(g(0)'g(0) - (L^{-1}g(0)'\iota)^2))}{(f(0)'f(0) - (L^{-1}f(0)'\iota)^2))} = 1 - \frac{L^{-1}\left(\sum_l g_l(0)^2 - \left(L^{-1}\sum_m g_m(0)\right)^2\right)}{L^{-1}\left(\sum_l f_l(0)^2 - (L^{-1}\sum_m f_m(0))^2\right)},$$

where f and g are the vector of functions f_l and g_l that are estimated using local linear regression and ι is an $L \times 1$ vector of ones.[2]

To construct confidence intervals for this estimate that correctly account for the discreteness of our outcome variable, we apply the delta method following Appendix B.1.1 of Armstrong and Kolesár (2018*a*). Let the numerator and denominator of ϕ be A and B, respectively. Then, $dA/dg = 2g(0)' - 2(L^{-1}g(0)'\iota)L^{-1}\iota'$ and $dB/df = 2f(0)' - 2(L^{-1}f(0)'\iota)L^{-1}\iota'$. The cross-derivatives are zero. Hence, $d\phi(f,g)/df = -d(AB^{-1})/df = -(dA/df)B^{-1}$ and $d\phi(f,g)/dg = -d(AB^{-1})/dg = -A(dB^{-1})/dg = A(B^{-2})dB/dg$.

Thus, our bias term will be $B = \sum_l |\phi_l' B_l|$, where B_l is the bias determined from the underlying estimation.

We next consider the covariance matrix Σ of our stacked f and g. Since we estimate each f_l and g_l separately, Σ is simply a diagonal matrix of the S_l^2 estimates for each $f_l(0)$ and $g_l(0)$ estimate. Hence, our variance estimate is $S^2 = \phi'(f,g)'\Sigma\phi'(f,g)$.

Finally, to calculate the confidence intervals around our estimate $\hat{T}(f,g)$, we follow Armstrong and Kolesár (2018*a*) and calculate the 95% confidence intervals around our estimate of the ratio as

$$\hat{T}(f,g) \pm \text{cv}_{0.95}(t) \cdot \hat{se},$$

where $t = B/S$ is our bias-sd ratio and $\hat{se} = \sqrt{S^2}$. We note that $\text{cv}_{0.95}(t)$ is the quantile of the folded normal distribution with mean equal to t (see the note in Table 1 of Armstrong and Kolesár (2018*a*)).

Shrinkage Estimators Due to smaller sample sizes, the locality-level estimates are noisier than estimates of the overall national effects (or counterfactuals). Hence, our estimates of γ_l, $y_l(65-)$, and $y_l(65+)$ have more inherent noise and variation than the true underlying estimates due to estimation error (in part due to smaller sample sizes). Here we provide additional details on the shrinkage estimator we use to address this.

Formally, using our estimates of state-level discontinuities as an example, we calculate the shrinkage estimator by assuming that the $\gamma_s \sim \mathcal{N}(\gamma_0, \sigma^2)$. We estimate these two parameters directly. Then, using the standard errors estimated for each γ_s, $\hat{\sigma}_s$, and following the standard James-Stein estimator approach (Morris, 1983), we construct $B = \frac{\hat{\sigma}^2}{\hat{\sigma}_s^2 + \hat{\sigma}^2}$, and our shrinkage estimator is $\tilde{\gamma}_s = B\hat{\gamma}_s + (1-B)\gamma_0$. The CZ-level counterfactuals in Figure 2, for example, are shrunk using this method.

B.2 Robustness checks

In this section, we discuss our approach to assessing the robustness of our results to alternative specifications and bandwidths. As discussed in Section B, our empirical methodology requires two tuning parameters: the bandwidth (standard regression discontinuity applications) and our

[2]Note that we additionally population-weight our estimates. We omit this notation here for simplicity's sake.

upper bound on the magnitude of the second derivative. In Figures A3 and A4, we present sensitivity tests for our main RD estimates for various outcome measures to the choice of bandwidth and our upper bound. Our results are qualitatively unchanged across our choice of bandwidth and upper bound. In Figures A5 and A6 we demonstrate that our estimated reductions in the variance of health insurance and collections debt are robust to alternative bound scaling factors and bandwidths.

In Appendix Table A1, we repeat our estimates for our consumer credit outcomes, using alternative RD methodologies. We do so in four ways. First, in Column 1, we replicate our main estimates from Figures 1 and A2. Second, we consider three parametric models, fitting a linear, quadratic and cubic model in age on either side of the discontinuity and estimating the jump at age 65. For inference, we use heteroskedasticity-robust standard errors. We report these estimates in Columns 2, 3 and 4. Third, we estimate the same models, but cluster on the running variable of age, as suggested in Lee and Card (2008) (and subsequently shown to have coverage issues in Kolesár and Rothe (2018)). We report these models in Columns 4, 5 and 6. Finally, we use local linear estimation using the `RDRobust` package from Calonico, Cattaneo and Titiunik (2015). We report this estimate in Column 8.

Our estimates are similar across various estimation methodologies. However, many outcomes do appear statistically significant when we cluster on the running variable, unlike in our main specification. This is likely due to incorrect coverage, as highlighted in Kolesár and Rothe (2018). When using heteroskedasticity-robust standard errors, there are also additional significant estimates, but fewer, and they are not consistent across various parametric forms. Our estimates are quite similar, qualitatively, to using the Calonico, Cattaneo and Titiunik (2015) method, but our preferred estimate's point estimate is larger in magnitude and the confidence interval is smaller for our collection estimates.

B.3 Forecasting the causal effects of Medicare by location

This section provides additional details about how we forecast the causal effects of Medicare by location. We are interested in the forecastable components of both γ_l and β_l, where β_l is our fuzzy-RD estimates of CZ-level reductions in collections debt *per newly-insured* (see Section 3 for details). We are interested in the best *predictions* of γ_l and β_l.

Ideally, each forecast would be the unbiased causal estimate for the location from our RD design. However, in many locations, the near-elderly population is small and the estimates are noisy. To reduce noise, we follow Chetty and Hendren (2018) and construct forecasts using a shrinkage estimator that combines our unbiased RD estimates and the predicted effect for each commuting zone based on its demographic and healthcare market characteristics. Since the dimension of our set of predictors, $\vec{X}_l$, is large (and many of the covariates are highly correlated), we use our Lasso predictions from Section 3.2 in order to minimize over-fitting.

We denote our predictions of γ_l and β_l estimated using our Lasso model as $\hat{\gamma}_l$ and $\hat{\beta}_l$, respectively. Briefly, the Lasso estimation procedure penalizes covariates and shrinks terms in the estimated ω_l towards zero, in order to minimize mean squared error. As a result, the estimation procedure will select a subset of the covariates in $\vec{X}_l$, to have non-zero parameters, and set the remaining parameters to zero. We implement this using a ten-fold cross-validation over the penalization parameter, implemented using R `glmnet` package.

To forecast the causal effects of Medicare by location, we then combine the Lasso estimates together with our RD estimates of γ_l order to construct the mean square error-minimizing forecast for each location, defined as $\hat{\gamma}_l^f$. This MSE-minimizing forecast is constructed using the following

formula (Chetty and Hendren, 2018):[3]

$$\hat{\gamma}_l^f = \left(\frac{\chi^2}{\chi^2 + s_l^2} (\gamma_l - \overline{\gamma}_l) + \frac{s_l^2}{\chi^2 + s_l^2} \tau (\hat{\gamma}_l - \overline{\hat{\gamma}}_l) \right) + \overline{\gamma}_l, \tag{4}$$

where $\overline{\gamma}_l$ is the average RD prediction across locations, $\overline{\hat{\gamma}}_l$ is the average Lasso prediction across locations, $\tau = Cov(\hat{\gamma}_l, \gamma_l)/Var(\hat{\gamma}_l)$ is the coefficient of a regression of γ_l on $\hat{\gamma}_l$, χ^2 is the residual place effect variation after subtracting off the variance due to estimation of γ_l, and s_l^2 the squared standard error of the γ_l. For the purposes of the shrinkage, we demean our estimates and then add the overall mean back, such that the shrinkage is around the variation around the overall mean. We estimate τ using linear regression of the demeaned values, and calculate χ^2 as

$$\chi^2 = Var(\gamma_l - \tau(\hat{\gamma}_l - \overline{\hat{\gamma}}_l)) - E(s_l^2),$$

where $E(s_l^2)$ is the average sampling variance across locations. In all calculations, we weight by the precision of the fixed effect estimates $(1/s_l^2)$ to maximize efficiency.

Note that this approach will shrink our estimates towards the predicted $\hat{\gamma}_l$ when the original estimate is noisy and the shrinkage will only occur if the lasso prediction has predictive power for γ_l. If this prediction has limited value, then τ will be zero, and the shrinkage will shrink towards the overall mean. By a similar argument, as s^2 goes to zero, the forecasted estimate will be exactly γ_l. We follow the same procedure to construct forecasts for β_l, defined as $\hat{\beta}_l^f$.

To calculate the prediction errors of the forecasts for Table A2, we follow Chetty and Hendren (2018), where the root mean-squared error of the prediction is:

$$\sqrt{e_l^2} = \sqrt{\frac{1}{\frac{1}{s_l^2} + \frac{1}{\chi^2}}}.$$

Note that as the variance for our unbiased estimate (s_l^2) grows, χ^2 places an upper bound on the size of the root MSE. In contrast, if the sampling error gets very small, the forecast will place all the weight on the unbiased estimate, and send the root MSE to zero.

B.4 Estimating the effects of Medicare eligibility before and after implementation of the ACA

We briefly describe the methods used to document differences in the effect of Medicare eligibility before and after the ACA. We also document our approach to quantifying the changes in health insurance and financial health for the near-elderly from the ACA.

To examine the relationship between Medicare eligibility, health insurance, and financial health before and the after the implementation of the ACA we re-estimate our primary specification separately, pre- and post-ACA:

$$y_{i,l,t}(\text{age}) = \gamma_T \times 1(\text{age} > 65) + f_T(\text{age}) \times 1(\text{age} \leq 65) + g_T(\text{age}) \times 1(\text{age} > 65) + \epsilon_{i,l,t}(\text{age}). \tag{5}$$

where T indexes the pre-ACA (2008-2013) and post-ACA (2014-2017) periods. The coefficients of interest are γ_T which measure the change in health insurance and financial strain at age 65 before

[3] See Appendix D of Chetty and Hendren (2018) for the explicit derivation of this approach. Our approach deviates from Chetty and Hendren (2018) in that we use the Lasso predicted estimate, rather than the estimated mean value of residents (as Chetty and Hendren (2018) do). This extension is discussed in their Appendix D. Additionally, since our estimates are not mean zero by construction, we demean our estimates for the purposes of the shrinkage, and then add the overall mean back in. Our approach is otherwise identical.

($T = 0$) and after ($T = 1$) the implementation of the ACA. As before, the above specification allows for flexible age trends on both sides of the discontinuity, with standard errors constructed using methods outlined in Kolesár and Rothe (2018) and discussed previously.

To quantify the changes in health insurance and financial health for the near-elderly from the ACA, we follow Duggan, Gupta and Jackson (2019) and estimate a regression discontinuity difference-in-differences ("difference-in-discontinuity") research design. Intuitively, this design exploits the fact that for 65-year-olds (and older), the expansion of the ACA was limited (compared to the near-elderly). To implement this approach, we construct $\Delta y_{i,l,t}(\text{age})) = y_{i,l,t}(\text{age})) - \bar{y}_{i,l,t,2010-2013}(age)$, where $\bar{y}_{i,l,t,2010-2013}(age)$ is the average outcome in a given location-age from 2010-2013. We then re-estimate our regression discontinuity approach using this modified outcome variable:

$$\Delta y_{i,l,t}(\text{age}) = \tilde{\gamma} \times 1(\text{age} > 65) + \tilde{f}(\text{age}) \times 1(\text{age} \leq 65) + \tilde{g}(\text{age}) \times 1(\text{age} > 65) + \tilde{\epsilon}_{i,l,t}. \quad (6)$$

with the standard errors constructed using methods outlined in Kolesár and Rothe (2018) and discussed previously.

B.5 Decomposing the change in forecast reductions in per capita collections before and after implementation of the ACA

In this section, we describe how we use our estimates to provide insight into why forecast reductions in collections have become increasingly concentrated in the Deep South. We are interested in understanding why the changes in the average CZ-level forecast from pre- to post-ACA differed between the South and other regions of the country.

To formally decompose this, we define the relative percentage change before and after the ACA , $\eta = \left(E(\gamma_l^{Post}) - E(\gamma_l^{Pre})\right) / E(\gamma_l^{Pre})$, for both regions, South and All Others. This change can be written as three parts: the change in the effect of Medicare on health insurance rates, the change in the effect of Medicare on collections debt per newly-insured, and the change in the covariance between the two. Formally,

$$\begin{aligned}
\eta &= \frac{\eta_1 + \eta_2 + \eta_3}{E(\gamma_l^{Pre})} \\
\eta_1 &= \left(E(\beta_l^{Post}) - E(\beta_l^{Pre})\right) E(\gamma_l^{h,Post}) \\
\eta_2 &= E(\beta_l^{Pre}) \left(E(\gamma_l^{h,Post}) - E(\gamma_l^{h,Pre})\right) \\
\eta_3 &= Cov(\beta_l^{Post}, \gamma_l^{h,Post}) - Cov(\beta_l^{Pre}, \gamma_l^{h,Pre})
\end{aligned}$$

This derivation follows from the fact that $E(\gamma_l) = E(\gamma_l^h \beta_l) = E(\gamma_l^h)E(\beta_l) + Cov(\gamma_l^h, \beta_l)$, where γ_l is the reduction in collections debt per capita at age 65, γ_l^h is the change in the insurance rate at age 65, and β_l is the reductions in debt collections *per newly-insured* at age 65. We then rearrange terms to derive the above expression. An important note is that since we are focusing on the forecasts, rather than the underlying parameters, there are small differences because we use the shrinkage estimates. E.g. $\gamma_l = \gamma_l^h \beta_l$, but we use $\hat{\gamma}_l$. As a result, it is useful to rewrite $\hat{\gamma}_l = \gamma_l + \epsilon_{\gamma,l}$, and note that $\hat{\gamma}_l = \gamma_l^h \beta_l + \epsilon_{\gamma,l}$. We can use these approximations to redefine our approximation in terms of the forecasted estimates, which will leave us with additional error terms. In our results, these terms are captured in our last decomposition piece, η_3.

For transparency, we present the underlying quantities in Appendix Table A5 and plot the three components of the decomposition (the ηs) in Panel B of Figure 5.

Appendix Figure A1: Changes in the distribution of collections debt at age 65

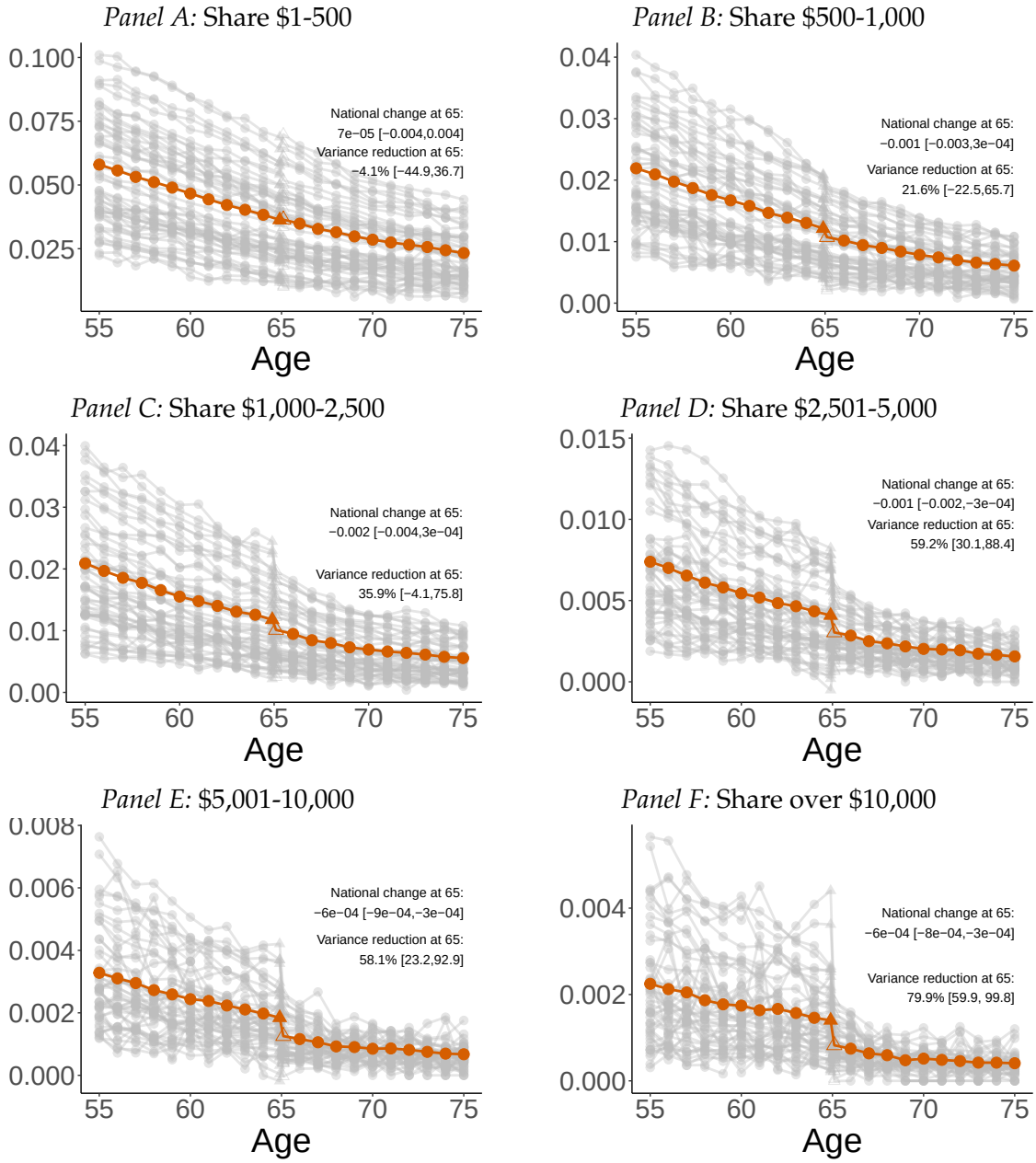

Note: This figure plots the effect of Medicare eligibility at age 65 on the distribution of new collections debts within the past year. A local linear regression is fit on each side of the Medicare eligibility threshold using methods from Kolesár and Rothe (2018). We include hollow points that are the predicted counterfactual outcomes with and without Medicare at 65. The blue hollow dot is the predicted outcome without Medicare at age 65 and the red hollow dot is the predicted consumer credit outcome with Medicare at age 65. Panel A plots the share of individuals with collections debt between $1-500 by age. Panel B plots the share of individuals with collections debt between $500-1,000 by age. Panel C plots the share of individuals with collections debt between $1,000-2,500 by age. Panel D plots the share of individuals with collections debt between $2,501-5,000 by age. Panel E plots the share of individuals with collections debt between $5,001-10,000 by age. Panel F plots the share of individuals with collections debt greater than $10,000 by age. The sample includes individuals who were age 55-75 between 2008 and 2017. See Section 2 for additional details on the outcomes and sample. Source: The financial health outcomes are based on 137,340,577 person-year observations from the New York Fed Consumer Credit Panel / Equifax, 2008-2017

Appendix Figure A2: Additional outcomes for changes in financial health at age 65

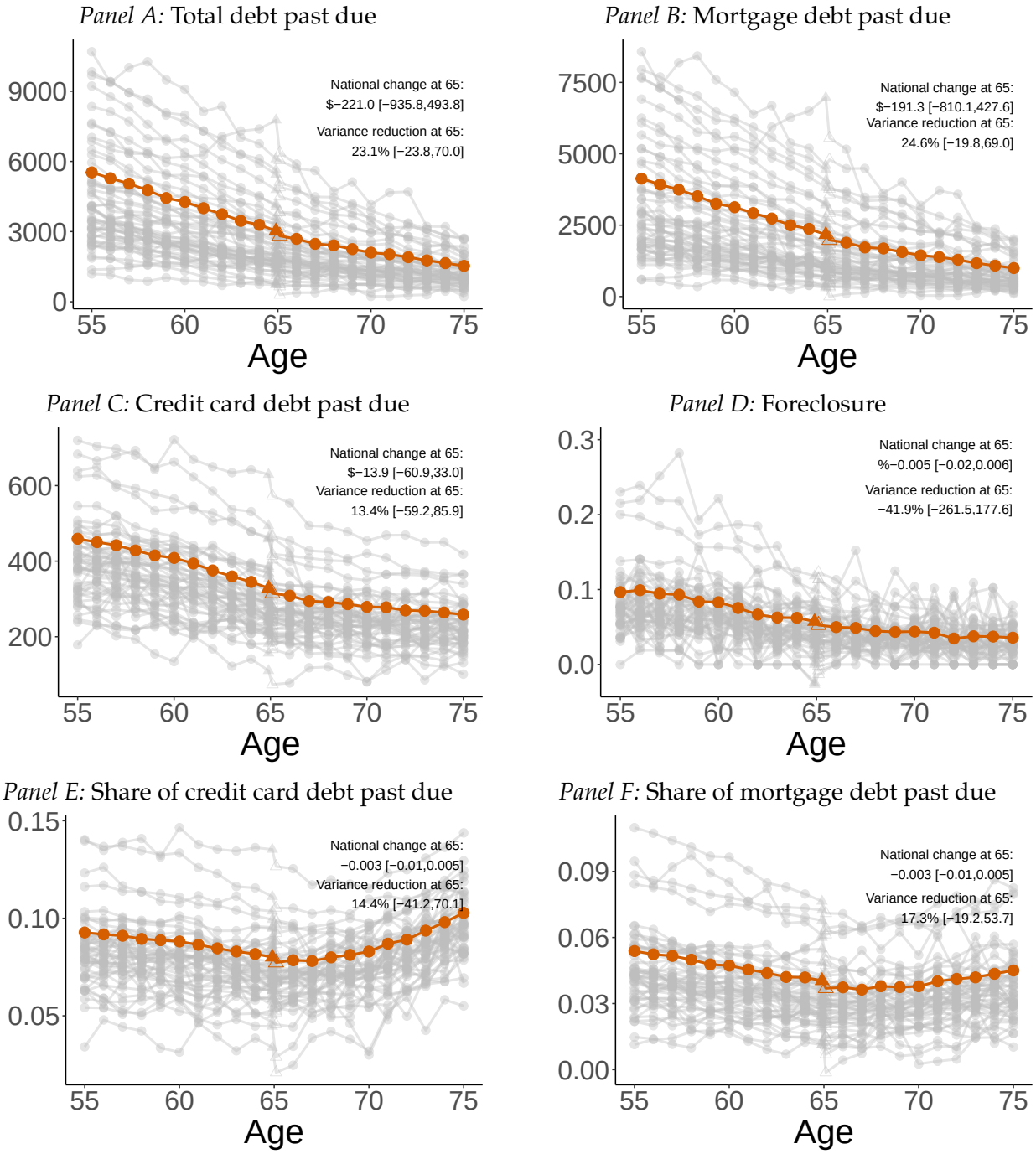

Note: This figure plots consumer credit outcomes by age. The horizontal axis denotes age in years. A local linear regression is fit on each side of the Medicare eligibility threshold using methods from Kolesár and Rothe (2018). We include hollow points that are the predicted counterfactual outcomes with and without Medicare at 65. The blue hollow dot is the predicted outcome without Medicare at age 65 and the red hollow dot is the predicted consumer credit outcome with Medicare at age 65. Panel A plots average amount of debt that is more than 30 days past due by age. Panel B plots the average amount of mortgage debt that is more than 30 days past due by age. Panel C plots the average amount of credit card debt that is more than 30 days past due by age. Panel D plots the share of individuals experiencing a foreclosure by age. Panel E reports the share of credit card that is more than 30 days past due. Panel F reports the share of mortgage debt that is more than 30 days past due. The share debt past due outcomes are calculated as the average individual debt past due, divided by the average total debt of all individuals of the same age living in that state. We divide by this average, rather than individuals' own debt levels, to avoid the divide-by-zero problem. The sample includes individuals who were age 55-75 between 2008 and 2017. See Section 2 for additional details on the outcomes and sample. Source: The financial health outcomes are based on 137,340,577 person-year observations from the New York Fed Consumer Credit Panel / Equifax, 2008-2017.

Appendix Figure A3: Robustness of Age RD Estimates to Bound Scaling Factor

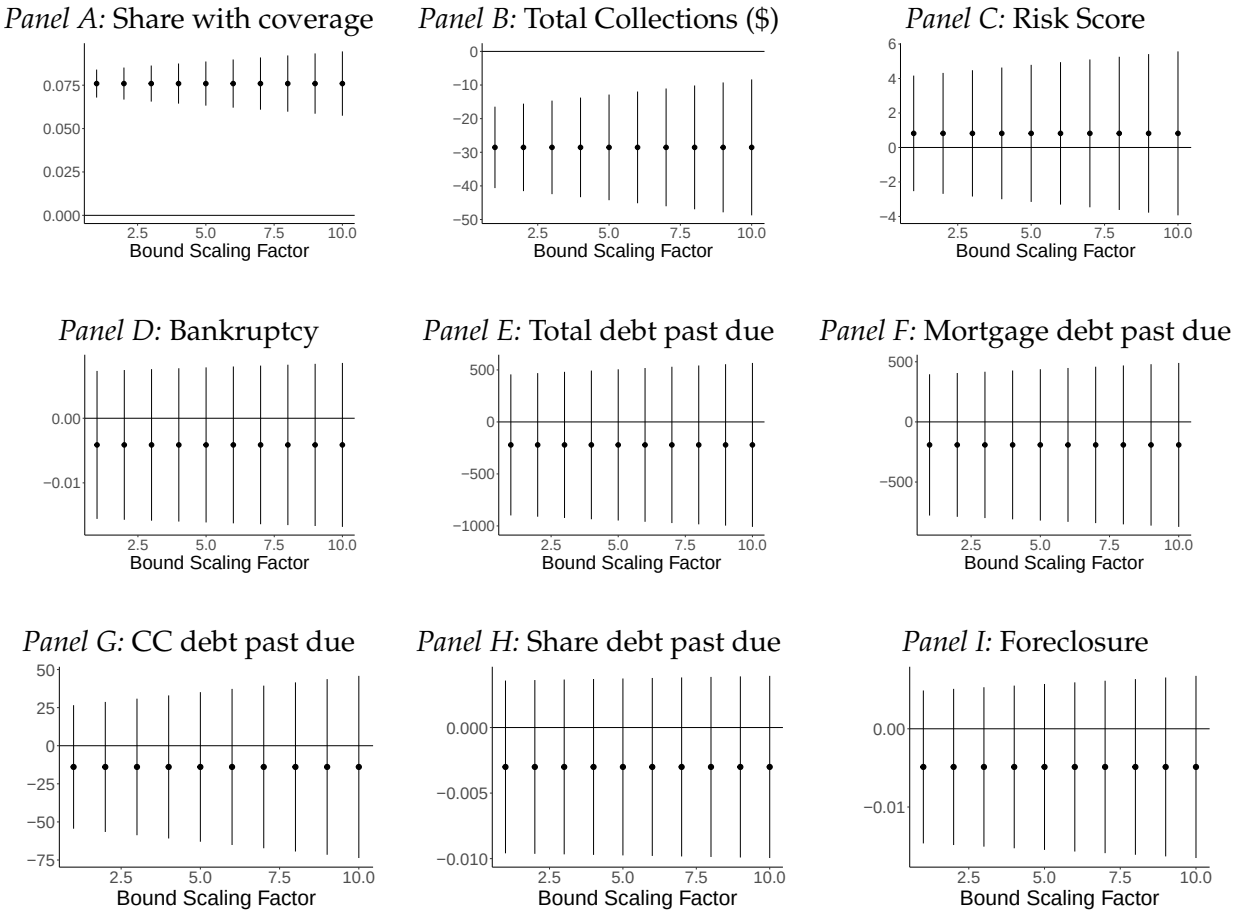

Note: This figure plots the robustness of our regression discontinuity estimates to the choice of the bound scaling factor used in the Kolesár and Rothe (2018) estimation procedure. Panel A plots the robustness of the share of the population with any coverage estimates. Panel B plots the robustness of the average debt in collections in dollars RD estimates. Panel C plots the robustness of the risk score RD estimates based on the Equifax Riskscore 3.0. Panel D plots the robustness of the bankruptcy RD estimates. Panel E plots the robustness of the average debt past due RD estimates. Panel F plots the robustness of the average mortgage debt past due RD estimates. Panel G plots the robustness of the average credit card debt past due RD estimates. Panel H plots the robustness of the share of debt past due RD estimates. Panel I plots the robustness of the foreclosure RD estimates. The sample includes individuals who were age 55-75 between 2008 and 2017. See Section 2 for additional details on the outcomes and sample. Source: The financial health outcomes are based on 137,340,577 person-year observations from the New York Fed Consumer Credit Panel / Equifax, 2008-2017.

Appendix Figure A4: Robustness of Age RD Estimates to Bandwidth Selection

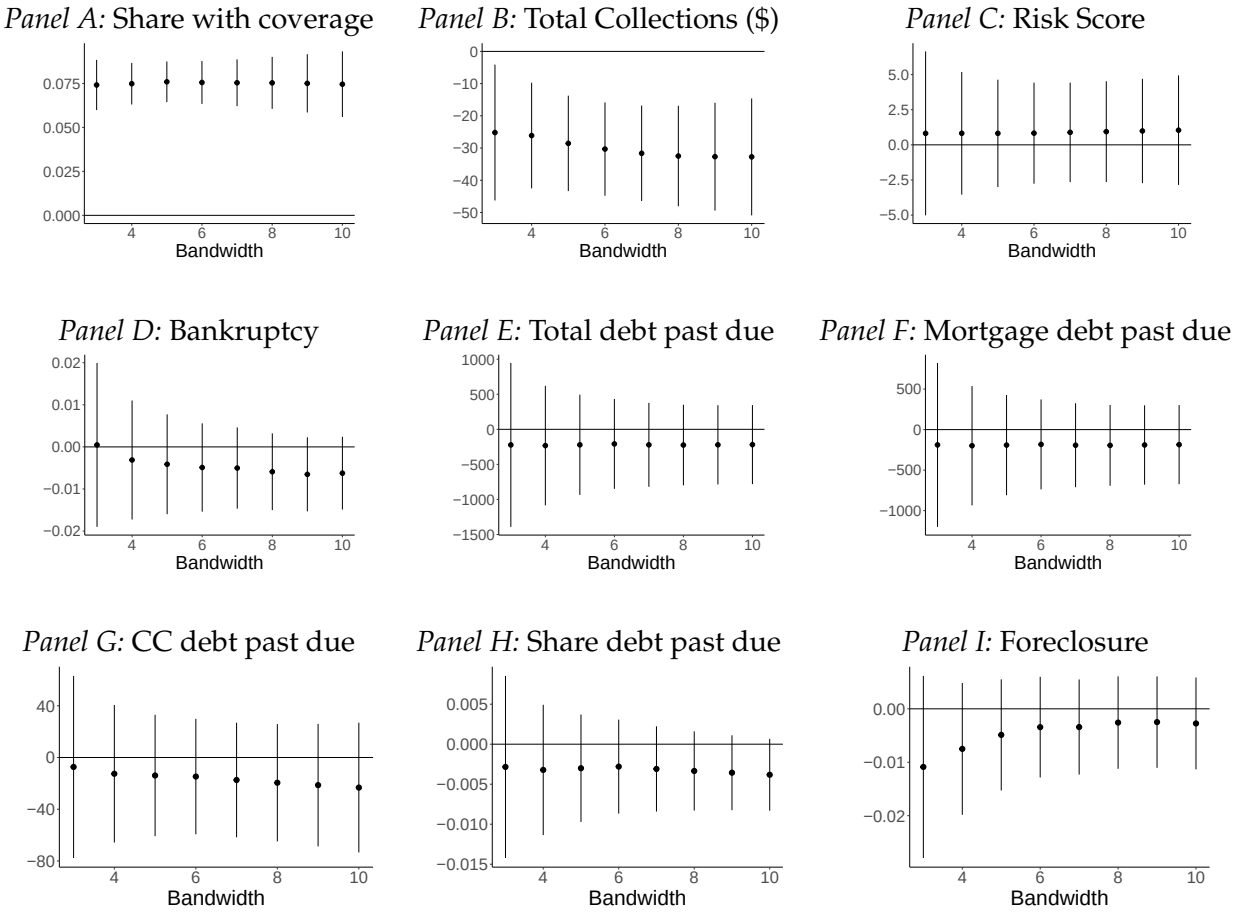

Note: This figure plots the robustness of our regression discontinuity estimates to the bandwidth selection used in the Kolesár and Rothe (2018) estimation procedure. Panel A plots the robustness of the share of the population with any coverage estimates. Panel B plots the robustness of the average debt in collections in dollars RD estimates. Panel C plots the robustness of the risk score RD estimates based on the Equifax Riskscore 3.0. Panel D plots the robustness of the bankruptcy RD estimates. Panel E plots the robustness of the average debt past due RD estimates. Panel F plots the robustness of the average mortgage debt past due RD estimates. Panel G plots the robustness of the average credit card debt past due RD estimates. Panel H plots the robustness of the share of debt past due RD estimates. Panel I plots the robustness of the foreclosure RD estimates. The sample includes individuals who were age 55-75 between 2008 and 2017. The regressions include 26,120,830 person-year-quarter observations for 2,977,952 unique individuals. See Section 2 for additional details on the outcomes and sample. Source: New York Fed Consumer Credit Panel / Equifax.

Appendix Figure A5: Robustness of Variance Reduction Estimates to Bound Scaling Factor

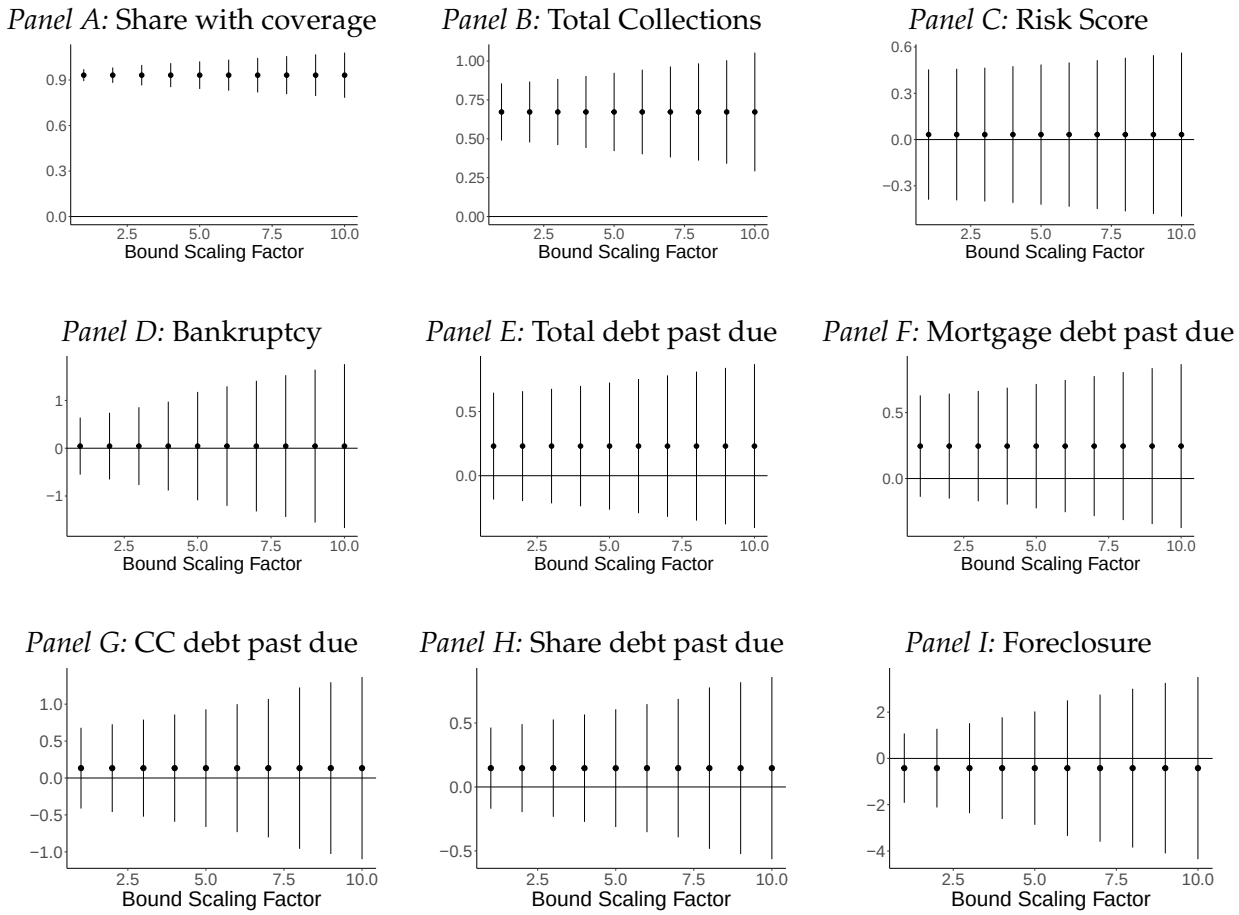

Note: This figure plots the robustness of our regression discontinuity estimates to the choice of the bound scaling factor used in the Kolesár and Rothe (2018) estimation procedure. Panel A plots the robustness of the share of the population with any coverage estimates. Panel B plots the robustness of the average debt in collections in dollars RD estimates. Panel C plots the robustness of the risk score RD estimates based on the Equifax Riskscore 3.0. Panel D plots the robustness of the bankruptcy RD estimates. Panel E plots the robustness of the average debt past due RD estimates. Panel F plots the robustness of the average mortgage debt past due RD estimates. Panel G plots the robustness of the average credit card debt past due RD estimates. Panel H plots the robustness of the share of debt past due RD estimates. Panel I plots the robustness of the foreclosure RD estimates. The sample includes individuals who were age 55-75 between 2008 and 2017. See Section 2 for additional details on the outcomes and sample. Source: The financial health outcomes are based on 137,340,577 person-year observations from the New York Fed Consumer Credit Panel / Equifax, 2008-2017.

Appendix Figure A6: Robustness of Variance Reduction Estimate to Bandwidth Selection

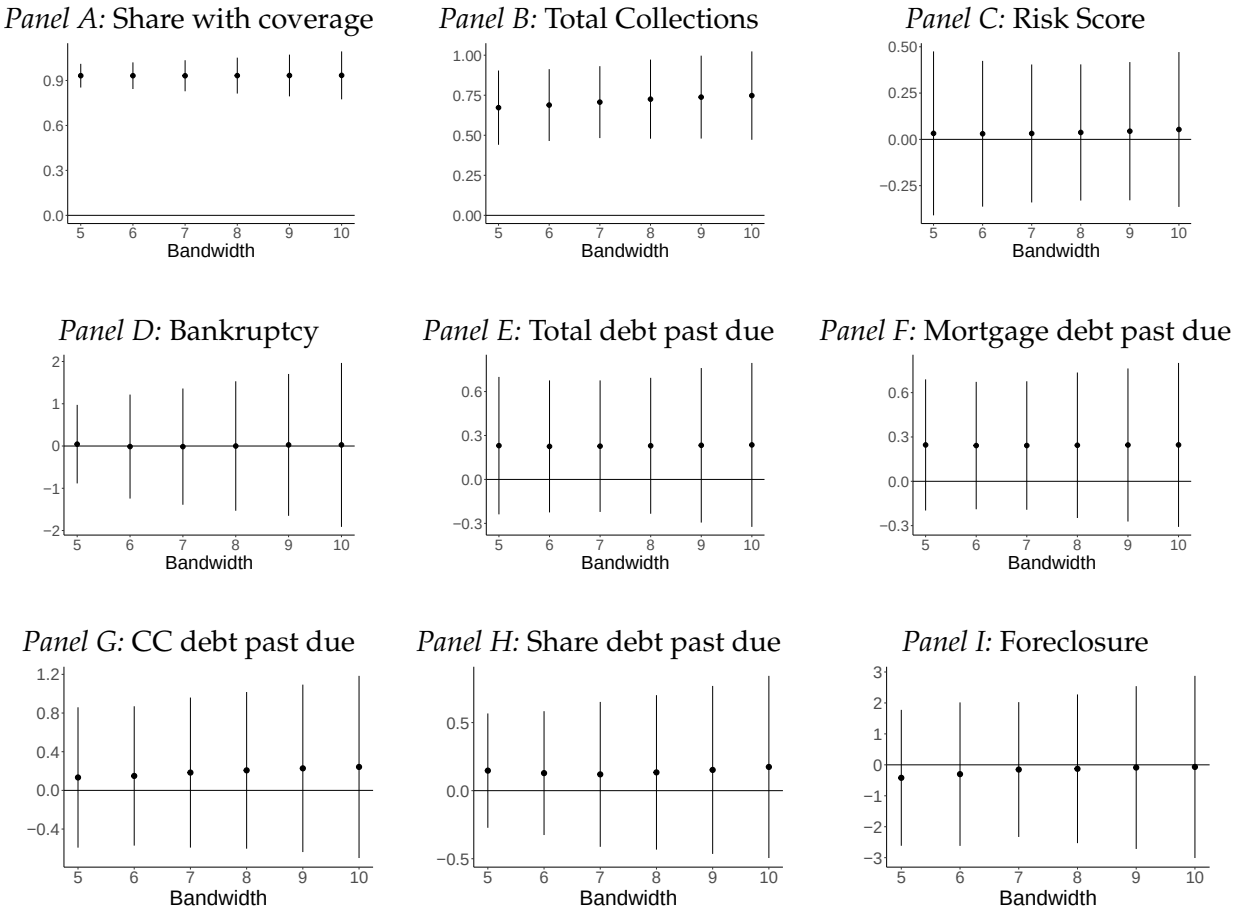

Note: This figure plots the robustness of our regression discontinuity estimates to the bandwidth selection used in the Kolesár and Rothe (2018) estimation procedure. Panel A plots the robustness of the share of the population with any coverage estimates. Panel B plots the robustness of the average debt in collections in dollars RD estimates. Panel C plots the robustness of the risk score RD estimates based on the Equifax Riskscore 3.0. Panel D plots the robustness of the bankruptcy RD estimates. Panel E plots the robustness of the average debt past due RD estimates. Panel F plots the robustness of the average mortgage debt past due RD estimates. Panel G plots the robustness of the average credit card debt past due RD estimates. Panel H plots the robustness of the share of debt past due RD estimates. Panel I plots the robustness of the foreclosure RD estimates. The sample includes individuals who were age 55-75 between 2008 and 2017. The regressions include 26,120,830 person-year-quarter observations for 2,977,952 unique individuals. See Section 2 for additional details on the outcomes and sample. Source: New York Fed Consumer Credit Panel / Equifax.

Appendix Figure A7: Smoothness of covariates at age 65

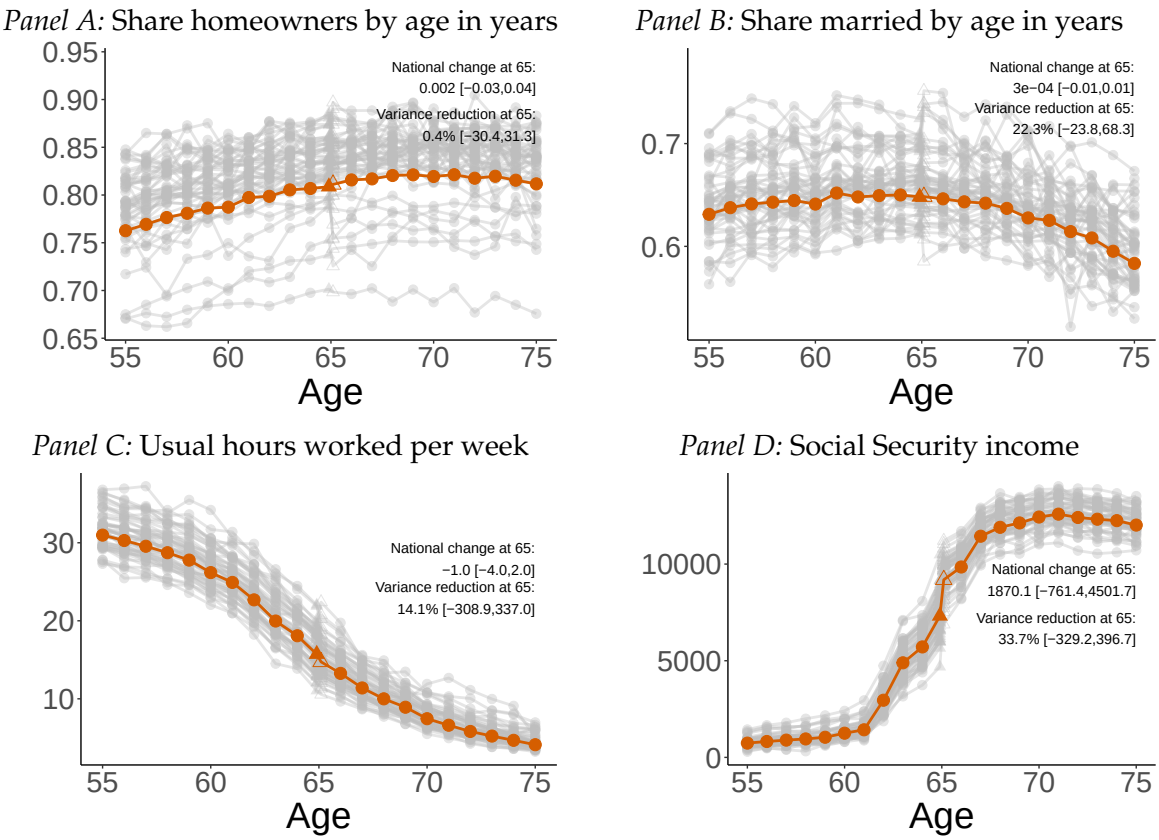

Note: This figure plots a series of individual covariates by age. The horizontal axis denotes age in years. A local linear regression is fit on each side of the Medicare eligibility threshold using methods from Kolesár and Rothe (2018). We include hollow points that are the predicted counterfactual outcomes with and without Medicare at 65. The blue hollow dot is the predicted covariate without Medicare and the red hollow dot is the predicted covariate with Medicare. Panel A plots homeownership rates by age. Panel B reports the share married by age. Panel C plots weekly hours worked by age. Panel D plots social security income by age. The sample includes individuals who were age 55-75 between 2008 and 2017. See Section 2 for additional details on the outcomes and sample. Source: American Community Survey, 2008-2017.

Appendix Figure A8: Covariate smoothness by state

Panel A: Homeowner

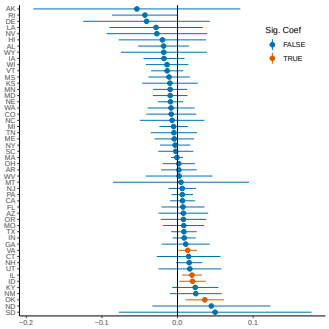

Panel B: Married

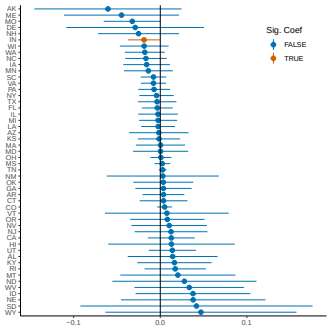

Panel C: Employed

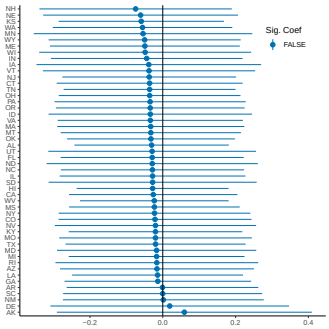

Panel D: Income

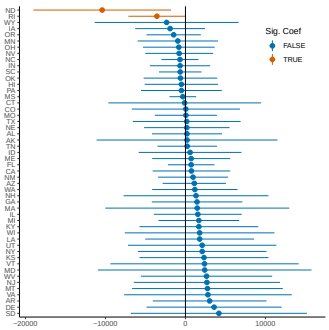

Panel E: Hours worked

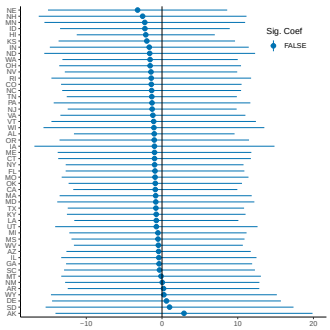

Panel F: Social Security Income

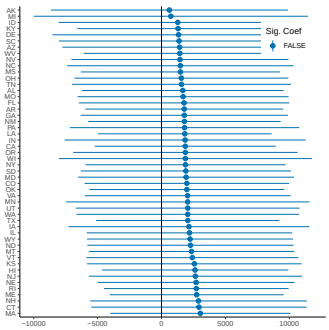

Note: This figure plots the estimated discontinuities at age 65 in individual covariates by state. A local linear regression is fit on each side of the Medicare eligibility threshold using methods from Kolesár and Rothe (2018). The red bars indicate statistically significant results at the 5% level. Panel A plots the estimated discontinuities in homeownership rates by state. Panel B plots the estimated discontinuities in marriage rates by state. Panel C plots the estimated discontinuities in employment by state. Panel D plots the estimated discontinuities in income by state. Panel E plots the estimated discontinuities in hours worked by state. Panel F plots the estimate discontinuities in social security income by state. The sample includes individuals who were age 55-75 between 2008 and 2017. See Section 2 for additional details on the outcomes and sample. Source: American Community Survey, 2008-2017.

Appendix Figure A9: Covariate smoothness by commuting zone

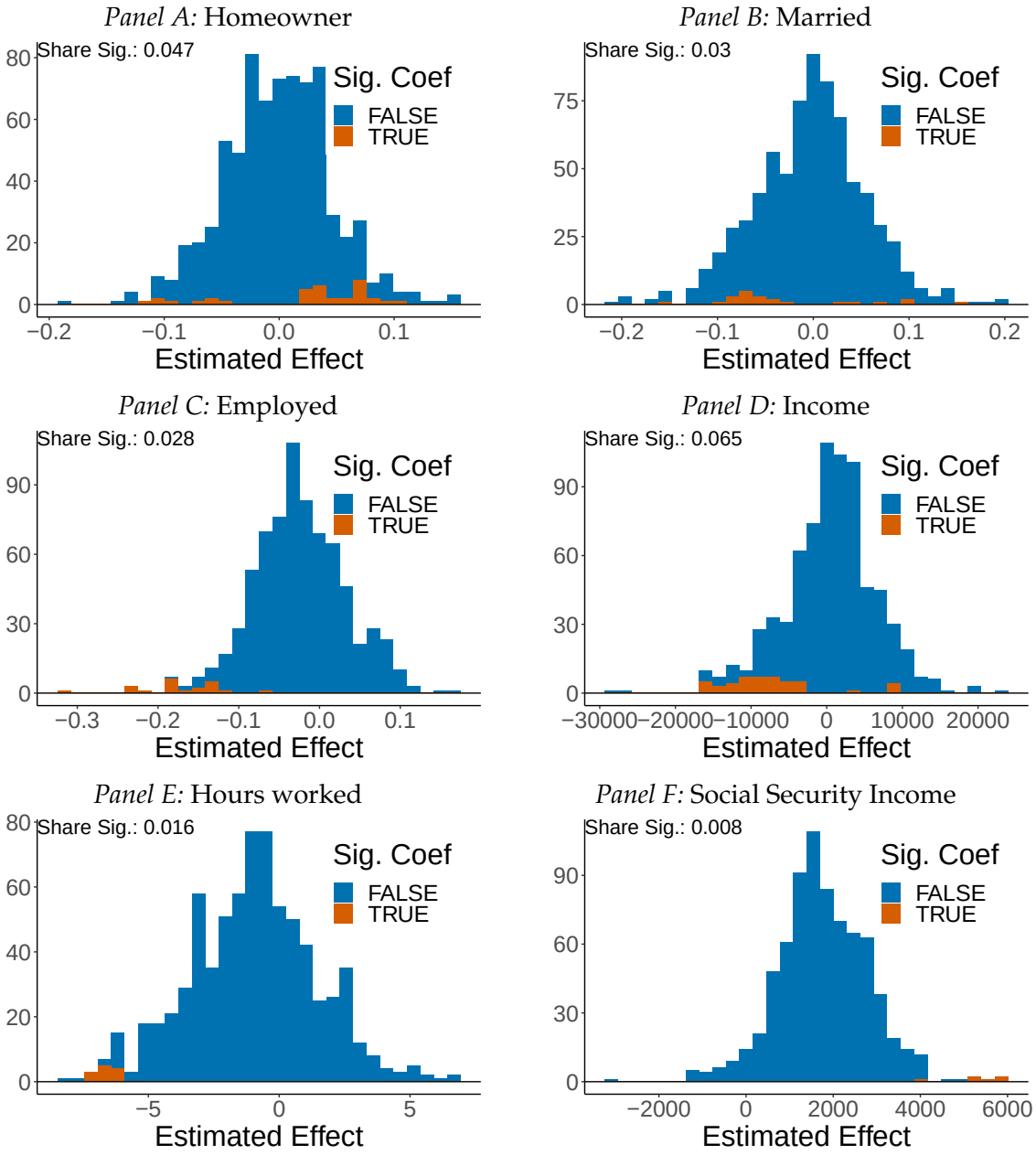

Note: This figure plots histograms of normalized estimated discontinuities at age 65 in individual covariates by commuting zone (CZ). A local linear regression is fit on each side of the Medicare eligibility threshold by CZ using methods from Kolesár and Rothe (2018). The red bars indicate statistically significant results at the 5% level. The blue bars indicate statistically insignificant results at the 5% level. Panel A plots the estimated discontinuities in homeownership rates by state. Panel B plots the estimated discontinuities in marriage rates by state. Panel C plots the estimated discontinuities in employment by state. Panel D plots the estimated discontinuities in income by state. Panel E plots the estimated discontinuities in hours worked by state. Panel F plots the estimate discontinuities in social security income by state. The sample includes individuals who were age 55-75 between 2008 and 2017. See Section 2 for additional details on the outcomes and sample. Source: American Community Survey, 2008-2017.

Appendix Figure A10: Consumer credit outcomes and uninsurance rates across states

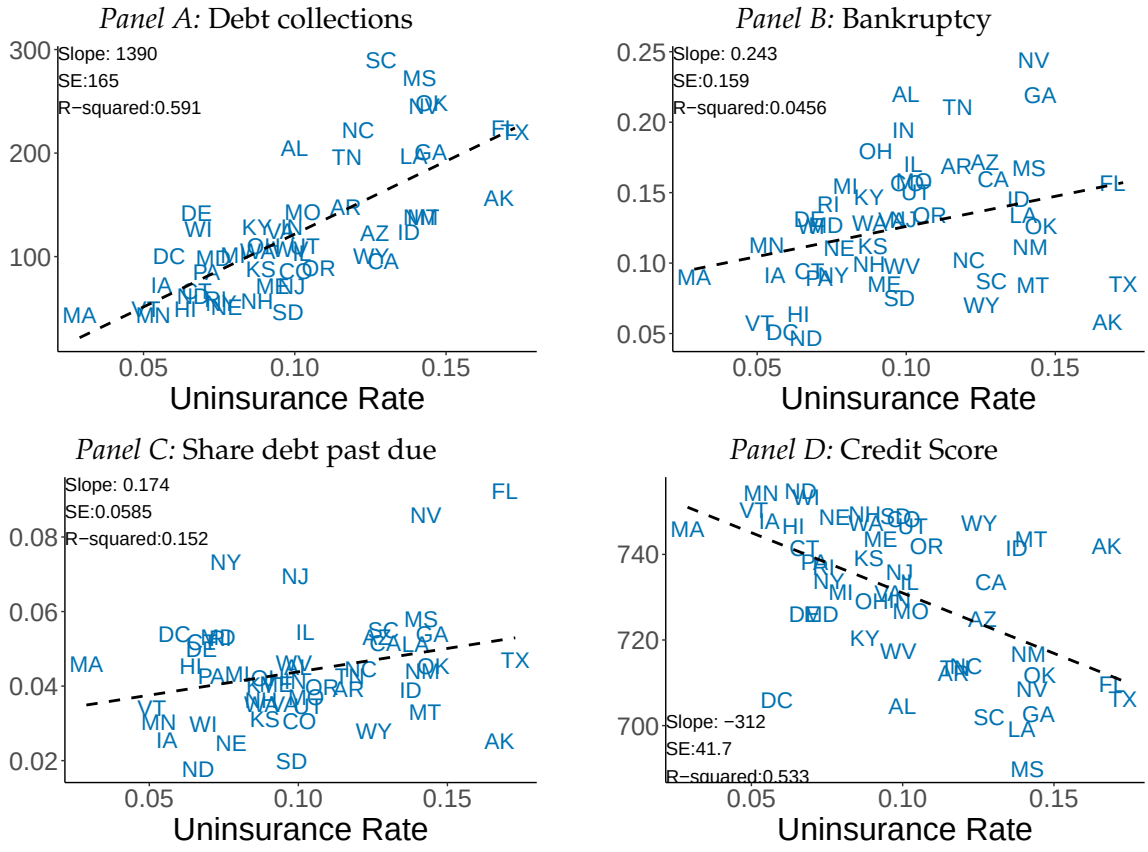

Note: This figure plots consumer credit outcomes against state uninsurance rates for individuals aged 55-64 years old. Panel A plots the dollar value of new collections debt reported on credit reports annually. Panel B plots the annual rate of new bankruptcies in percentage points. Panel C plots the share of debt that is more than 30 days past due. The share debt past due is calculated as the average individual's debt more than 30 days past due, divided by the average total debt of all individuals of the same age living in that state. Panel D plots credit score data using the Equifax Risk Score 3.0. See Section 2 for additional details on the outcomes and sample. Source: Consumer credit outcomes are based on 137,340,577 person-year observations from the New York Fed Consumer Credit Panel / Equifax, 2008-2017. State-level uninsurance rates are from the American Community Survey, 2008-2017.

Appendix Figure A11: Effect of Medicare eligibility on the level of collections debt at age 65 vs. effects on insurance

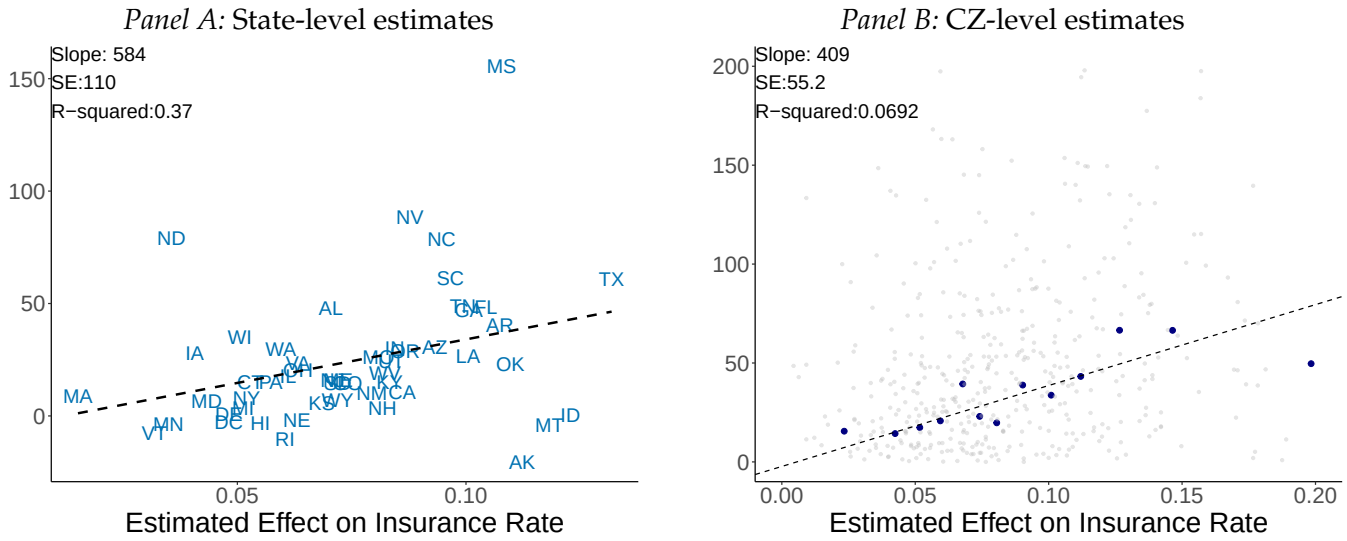

Note: This figure plots point estimates of the reduction in the flow of newly-reported collections debt (within the past year) and the increase in the insurance rate at age 65 based on local linear regressions, done separately by state and commuting zone (CZ), using the methods from Kolesár and Rothe (2018). Panel A plots state-level estimates. Panel B plots CZ-level estimates, where the dark points are binned averages constructed using the `binsreg` command from Cattaneo et al. (2019). The horizontal axes are the estimated effect on the insurance rate at age 65 by locality. The vertical axes are the reduction in the flow of collections debt at age 65 by locality. Source: Consumer credit outcomes are based on 137,340,577 person-year observations from the New York Fed Consumer Credit Panel / Equifax, 2008-2017. State-level uninsurance rates are from the American Community Survey, 2008-2017.

Appendix Figure A12: Correlates with reduction in collections debt at age 65, with Fixed Effects

Panel A: Area-level demographic characteristics

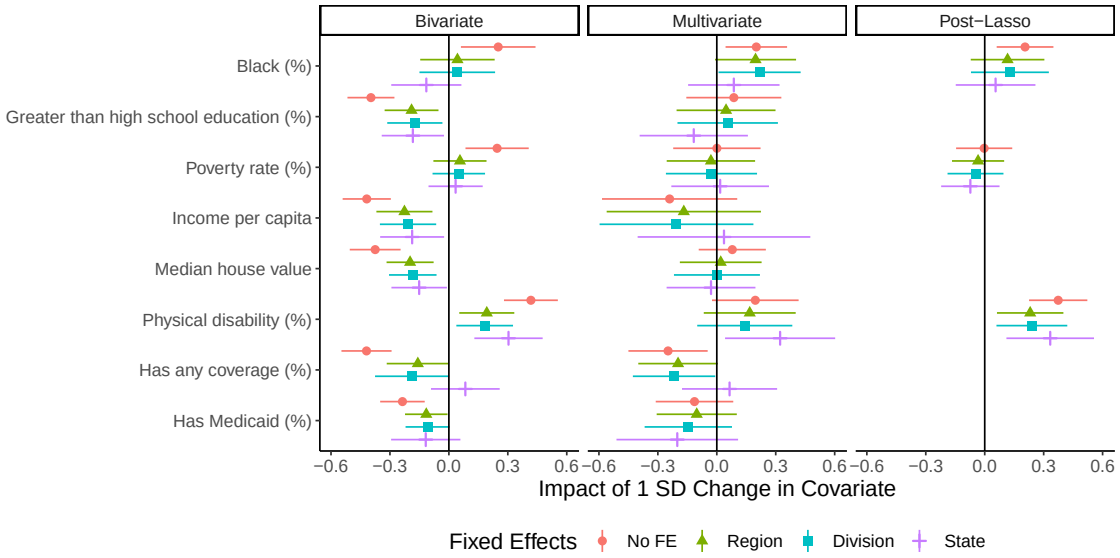

Panel B: Healthcare market characteristics

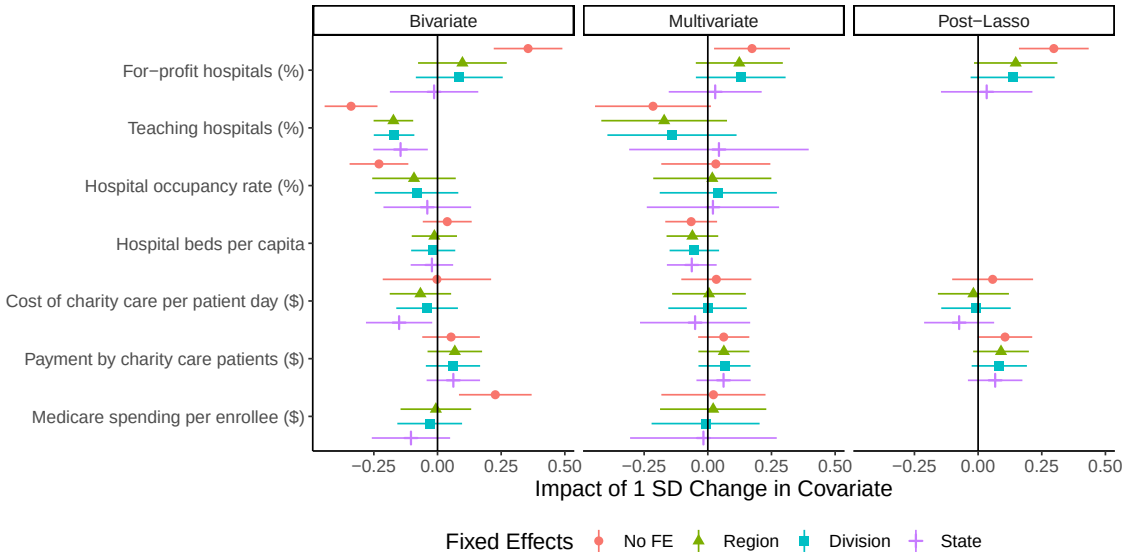

Note: This figure plots bivariate OLS regression results (left panel), multivariate OLS regression results (center panel), and post-Lasso multivariate regression results (right panel) of CZ-level estimated reductions in collections debt per capita on a set of CZ-level characteristics. We standardize all the variables so the coefficients reflect the strength of the association between a one standard deviation change in the covariate and the estimated reduction in collections debt at age 65. The horizontal bars are 95% confidence intervals. The multivariate OLS regression results and post-Lasso multivariate regression results are both run on the full set of characteristics in Panels A and B. For post-Lasso, we first estimate a Lasso regression on the full set of characteristics and then report the results of multivariate OLS run on the characteristics chosen by the Lasso regression. For each correlate we report our primary results where there are area-level fixed effects (termed "No FE") and then results where we include fixed effects for Census Region, Census Division, and state, respectively. Tabular versions of these results are in Table A4. Source: Consumer credit outcomes are based on 137,340,577 person-year observations from the New York Fed Consumer Credit Panel / Equifax, 2008-2017. CZ-level uninsurance rates are from the American Community Survey, 2008-2017. Healthcare market characteristics are from the Healthcare Cost Report Information System (HCRIS) and the Dartmouth Atlas. For additional details on the data see Section 2.

Appendix Figure A13: Effect of Medicare eligibility on per-capita collections debt vs. per-newly insured collections debt at the CZ-level

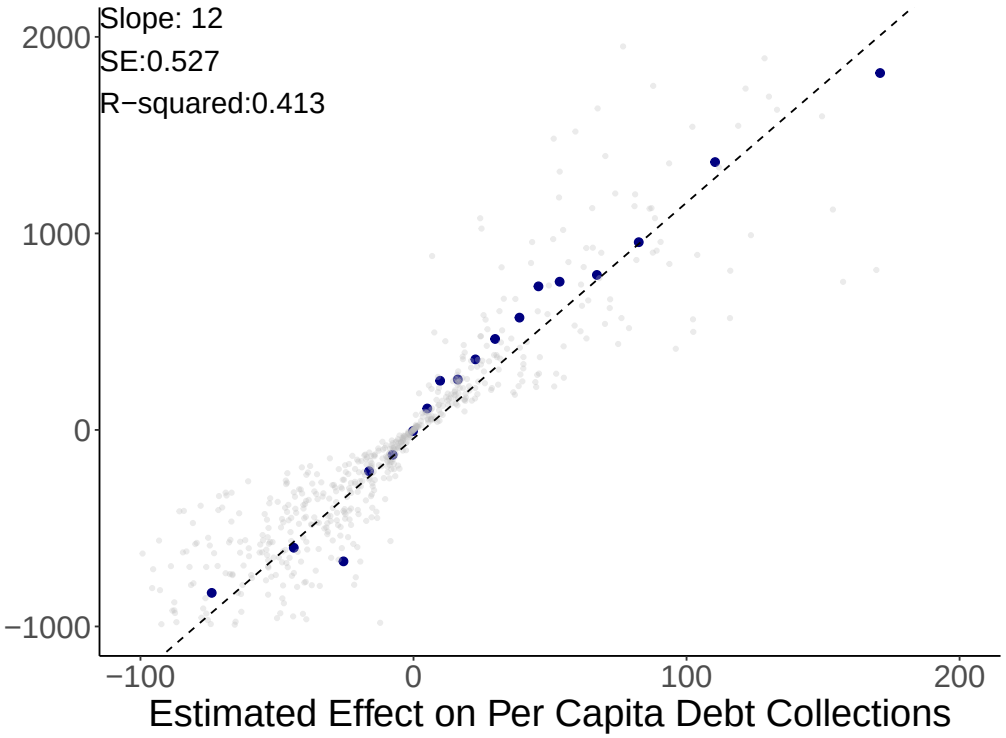

Note: This figure plots point estimates of the reduction in the flow of per-capita collections debt (within the past year) vs. point estimates of the reduction in the flow of per-capita collections debt (within the past year) per newly-insured. The estimates are based on local linear regressions, done separately by commuting zone (CZ), using the methods from Kolesár and Rothe (2018). The dark points are binned averages constructed using the `binsreg` command from Cattaneo et al. (2019). The horizontal axis is the estimated effect on per capita debt collections at age 65 by CZ. The vertical axis is the estimated reduction in the flow of collections debt per newly-insured at age 65 by CZ. Source: Consumer credit outcomes are based on 137,340,577 person-year observations from the New York Fed Consumer Credit Panel / Equifax, 2008-2017. State-level uninsurance rates are from the American Community Survey, 2008-2017.

Appendix Figure A14: Forecasts of causal reductions in collections debt from expanding health insurance to the near-elderly by commuting zone

Panel A: Pre-ACA, 2008-2013

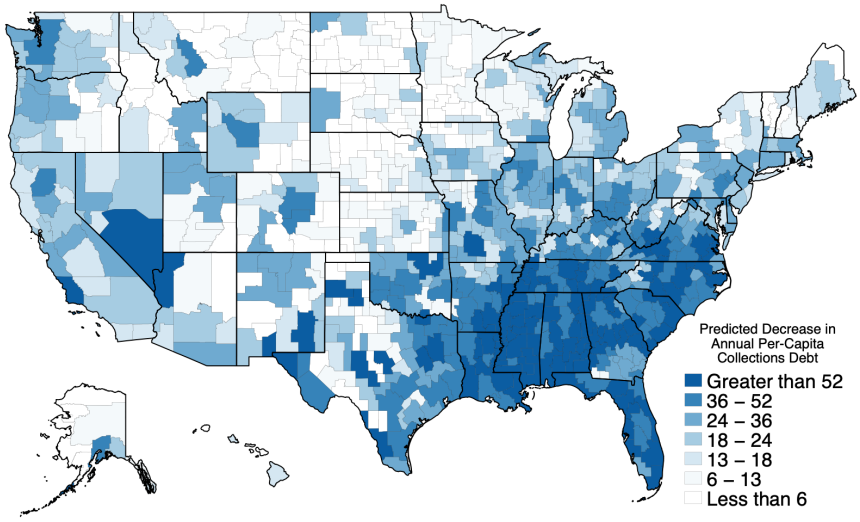

Panel B: Post-ACA, 2014-2017

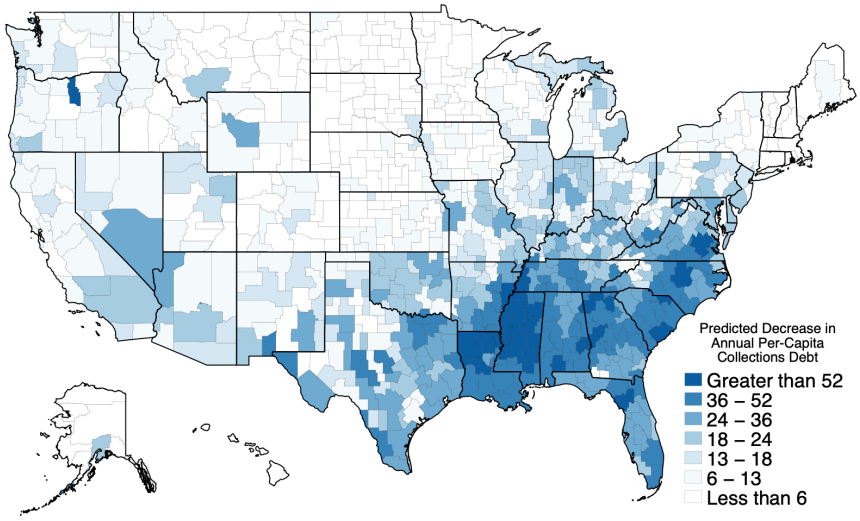

Note: This figure plots mean square error (MSE)-minimizing forecasts of the reductions in collections debt per capita in the pre-ACA (Panel A) and post-ACA period (Panel B). We construct the MSE-minimizing forecasting by first running a Lasso regression to predict the CZ-level reductions in collections debt per capita separate for each period. This generates a prediction for each CZ in each period, which we call $\hat{\gamma}_l$. Following Chetty and Hendren (2018) we then combine the $\hat{\gamma}_l$ estimates with our estimates of γ_l to construct the mean square error-minimizing forecast for each commuting zone in each period, γ_l^f. Source: Consumer credit outcomes are based on 137,340,577 person-year observations from the New York Fed Consumer Credit Panel / Equifax, 2008-2017. CZ-level uninsurance rates are from the American Community Survey, 2008-2017. Healthcare market characteristics are from the Healthcare Cost Report Information System (HCRIS) and the Dartmouth Atlas. For additional details on the data see Section 2..

Appendix Figure A15: Counterfactual health insurance rates by commuting zone at age 65 without Medicare, pre- and post-ACA

Panel A: Pre-ACA, 2008-2013

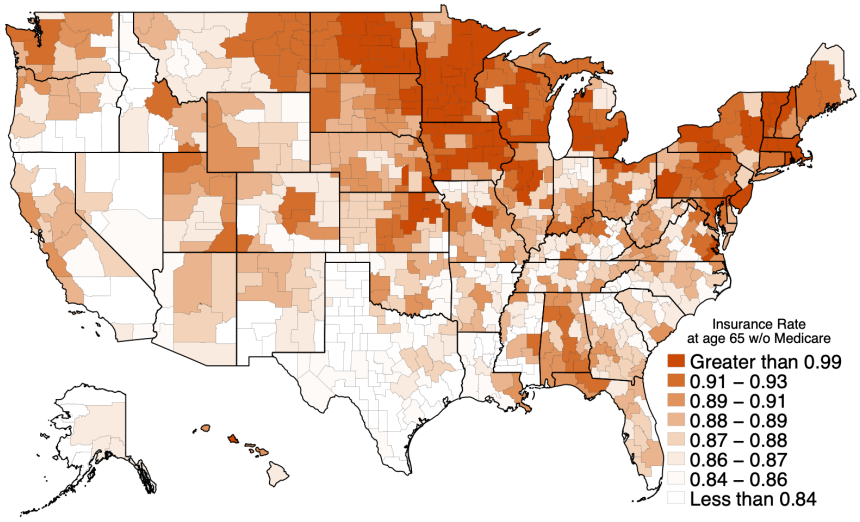

Panel B: Post-ACA, 2014-2017

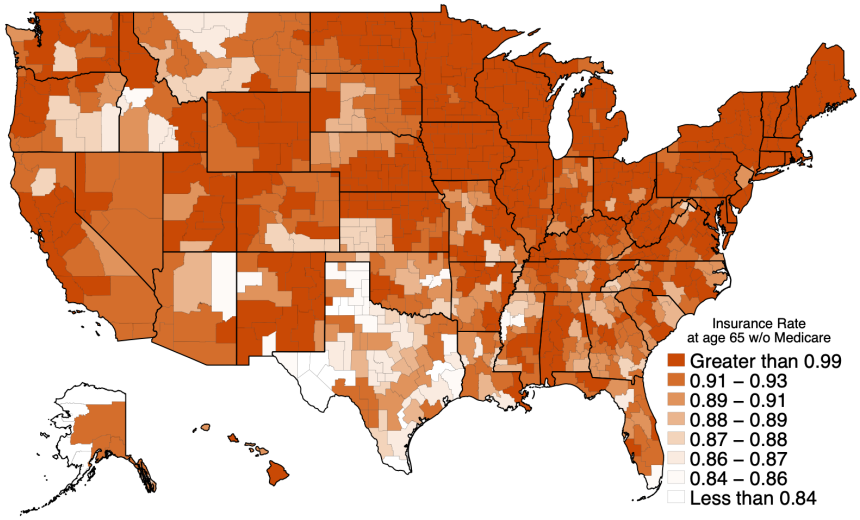

Note: This figure plots our counterfactual estimates of the share of the population with health insurance coverage at age 65, without Medicare, before and after the full implementation of the Affordable Care Act in 2014. The counterfactuals are based on local linear regressions, done separately by commuting zone, using the methods from Kolesár and Rothe (2018). These estimates are then shrunk using empirical Bayes, described in Section B. Panel A. presents the counterfactuals from the pre-ACA period, 2008-2013. Panel B. presents the counterfactuals from the post-ACA period, 2014-2017. Darker shading corresponds to states with higher counterfactual health insurance rates. Source: CZ-level uninsurance rates are from the American Community Survey, 2008-2017.

Appendix Figure A16: Difference-in-discontinuities estimates of increases in the near-elderly health insurance rate due to the ACA

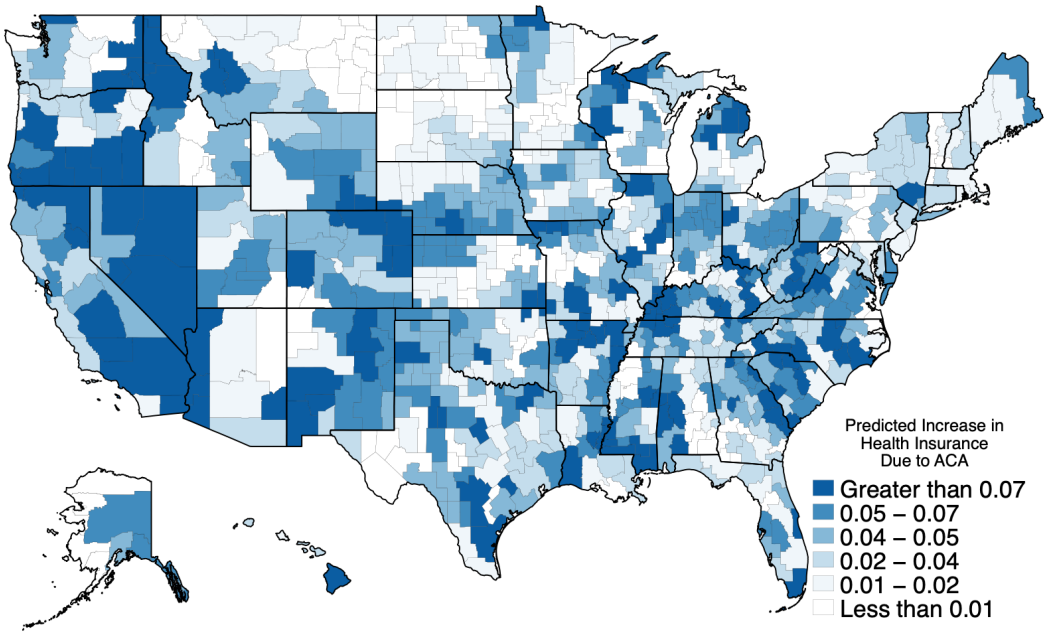

Note: This figure plots CZ-level estimates of the increase in health insurance coverage due to the Affordable Care Act using a difference-in-discontinuities design similar to Duggan, Gupta and Jackson (2019). We compare the discontinuity in health insurance at age 65 in the post-ACA period (2014-2017) to the discontinuity in health insurance at age 65 prior to its full implementation (2008-2013). CZ-level uninsurance rates are from the American Community Survey, 2008-2017.

Appendix Figure A17: Forecasts of causal reductions in collections debt per newly-insured near-elderly person by commuting zone, pre- and post-ACA

Panel A: Pre-ACA, 2008-2013

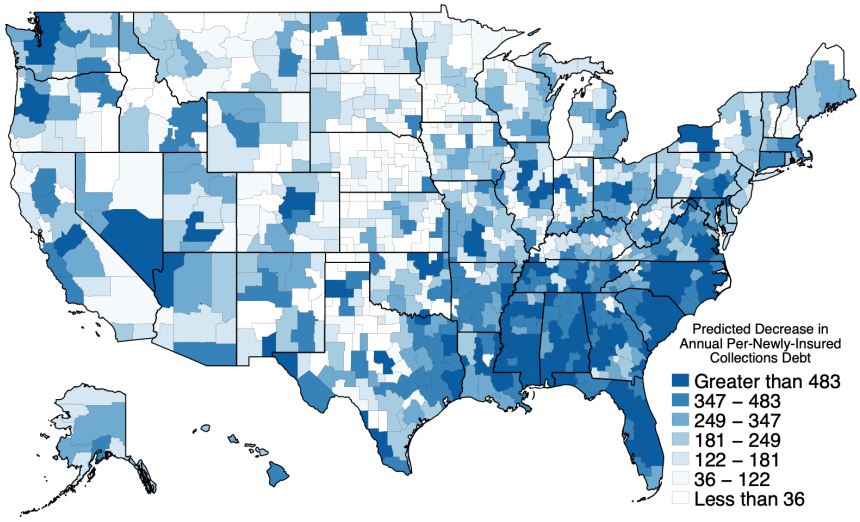

Panel B: Post-ACA, 2014-2017

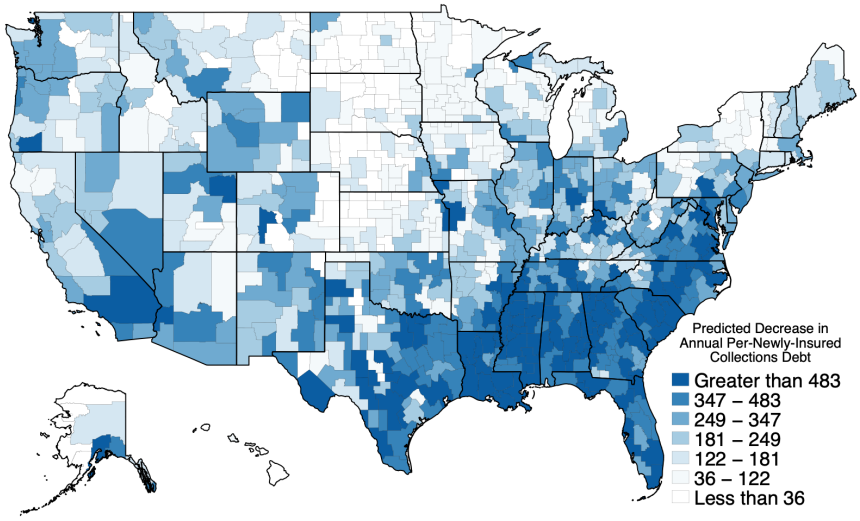

Note: This figure plots mean square error (MSE)-minimizing forecasts of the reductions in collections debt per newly-insured for the pre-ACA period (Panel A) and post-ACA period (Panel B). We construct the MSE-minimizing forecasting by first running a Lasso regression to predict the CZ-level reductions in collections debt per newly-insured. This generates a prediction for each CZ, which we call $\hat{\beta}_l$. Following Chetty and Hendren (2018) we then combine the $\hat{\beta}_l$ estimates with our estimates of β_l to construct the mean square error-minimizing forecast for each commuting zone, β_l^f. Source: Consumer credit outcomes are based on 137,340,577 person-year observations from the New York Fed Consumer Credit Panel / Equifax, 2008-2017. State-level uninsurance rates are from the American Community Survey, 2008-2017. Healthcare market characteristics are from the Healthcare Cost Report Information System (HCRIS) and the Dartmouth Atlas. For additional details on the data see Section 2.

Appendix Table A1: Robustness of estimated changes in financial outcomes at age 65

	Main Estimate	Linear with robust SEs	Quad. with robust SEs	Cubic. with robust SEs	Linear with clustered SEs	Quad. with clustered SEs	Cubic. with clustered SEs	Local linear with rdrobust
	(1)	(2)	(3)	(4)	(5)	(6)	(7)	(8)
Share with any coverage	0.076∗	0.073∗	0.077∗	0.074∗	0.073∗	0.077∗	0.074∗	0.073∗
	(0.004)	(0.002)	(0.004)	(0.007)	(0.002)	(0.001)	(0.002)	(0.01)
	[0.064,	[0.069,	[0.069,	[0.06,	[0.07,	[0.075,	[0.071,	[0.053,
	0.087]	0.078]	0.086]	0.088]	0.077]	0.08]	0.078]	0.093]
Debt in collections	−28.546∗	−32.981∗	−32.121∗	−23.58∗	−32.981∗	−32.121∗	−23.58∗	−21.558∗
	(6.813)	(2.578)	(4.407)	(7.467)	(2.212)	(2.498)	(2.549)	(10.83)
	[−43.355,	[−38.034,	[−40.76,	[−38.216,	[−37.317,	[−37.018,	[−28.577,	[−42.783,
	−13.737]	−27.928]	−23.483]	−8.945]	−28.645]	−27.224]	−18.584]	−0.332]
Credit score	0.818	1.199	0.645	0.682	1.199∗	0.645∗	0.682∗	0.795
	(1.943)	(0.87)	(1.515)	(2.57)	(0.437)	(0.135)	(0.108)	(3.663)
	[−3.001,	[−0.506,	[−2.324,	[−4.357,	[0.342,	[0.381,	[0.471,	[−6.384,
	4.637]	2.905]	3.614]	5.72]	2.057]	0.909]	0.892]	7.975]
Bankruptcy (pp)	−0.004	−0.006	−0.008	0.005	−0.006∗	−0.008	0.005	0.003
	(0.007)	(0.003)	(0.006)	(0.01)	(0.003)	(0.005)	(0.006)	(0.013)
	[−0.016,	[−0.012,	[−0.019,	[−0.014,	[−0.011,	[−0.017,	[−0.006,	[−0.023,
	0.008]	0.001]	0.003]	0.024]	0]	0.001]	0.016]	0.029]
Share employed	−0.029	−0.089∗	−0.002	−0.016	−0.089∗	−0.002	−0.016	−0.039
	(0.008)	(0.004)	(0.008)	(0.014)	(0.017)	(0.01)	(0.014)	(0.022)
	[−0.096,	[−0.097,	[−0.018,	[−0.043,	[−0.122,	[−0.022,	[−0.043,	[−0.083,
	0.038]	−0.08]	0.014]	0.01]	−0.055]	0.018]	0.01]	0.004]
Income	880.67	458.575	1572.808	343.741	458.575	1572.808∗	343.741	997.591
	(1322.697)	(749.423)	(1315.303)	(2235.622)	(244.825)	(285.332)	(333.556)	(4308.174)
	[−2002.838,	[−1010.295,	[−1005.185,	[−4038.078,	[−21.281,	[1013.557,	[−310.03,	[−7446.274,
	3764.179]	1927.445]	4150.801]	4725.559]	938.432]	2132.06]	997.511]	9441.457]
Total debt past due	−220.973	−213.784	−230.164	−200.976	−213.784∗	−230.164∗	−200.976∗	−233.868
	(404.833)	(139.794)	(240.424)	(412.141)	(38.637)	(53.615)	(52.082)	(746.706)
	[−935.78,	[−487.78,	[−701.396,	[−1008.772,	[−289.513,	[−335.25,	[−303.057,	[−1697.385,
	493.833]	60.212]	241.067]	606.82]	−138.055]	−125.079]	−98.895]	1229.649]
Mortgage debt past due	−191.289	−176.85	−207.937	−177.245	−176.85∗	−207.937∗	−177.245∗	−195.622
	(350.784)	(120.781)	(206.156)	(354.14)	(30.91)	(44.385)	(46.654)	(634.81)
	[−810.149,	[−413.58,	[−612.002,	[−871.359,	[−237.433,	[−294.932,	[−268.687,	[−1439.827,
	427.571]	59.881]	196.128]	516.87]	−116.266]	−120.942]	−85.803]	1048.583]
Credit card debt past due	−13.922	−27.734∗	−11.793	−6.079	−27.734∗	−11.793∗	−6.079	−4.517
	(23.341)	(9.16)	(16.058)	(27.349)	(4.22)	(3.959)	(4.492)	(49.812)
	[−60.867,	[−45.688,	[−43.265,	[−59.683,	[−36.005,	[−19.552,	[−14.883,	[−102.146,
	33.023]	−9.781]	19.68]	47.524]	−19.464]	−4.033]	2.724]	93.112]
Foreclosure	−0.005	−0.003	−0.001	−0.01	−0.003	−0.001	−0.01∗	−0.015
	(0.006)	(0.003)	(0.005)	(0.008)	(0.002)	(0.004)	(0.004)	(0.014)
	[−0.015,	[−0.009,	[−0.011,	[−0.026,	[−0.007,	[−0.008,	[−0.017,	[−0.042,
	0.006]	0.002]	0.008]	0.006]	0]	0.006]	−0.003]	0.011]
Share of mortgage debt past due	−0.003	−0.005∗	−0.003	−0.003	−0.005∗	−0.003∗	−0.003∗	−0.003
	(0.005)	(0.002)	(0.003)	(0.005)	(0.001)	(0.001)	(0.001)	(0.008)
	[−0.012,	[−0.008,	[−0.008,	[−0.012,	[−0.006,	[−0.005,	[−0.005,	[−0.019,
	0.005]	−0.002]	0.002]	0.006]	−0.003]	−0.001]	−0.001]	0.013]
Share of cc debt past due	−0.003	−0.008∗	−0.001	−0.001	−0.008∗	−0.001∗	−0.001	−0.001
	(0.004)	(0.002)	(0.003)	(0.005)	(0.002)	(0.001)	(0.001)	(0.01)
	[−0.011,	[−0.011,	[−0.007,	[−0.011,	[−0.011,	[−0.002,	[−0.002,	[−0.02,
	0.005]	−0.004]	0.005]	0.009]	−0.004]	0]	0.001]	0.018]

Note: This table reports the sensitivity of our main regression discontinuity estimates to alternative specifications. Column 1 reports the point estimate, standard error, and bias-adjusted 95% confidence interval from a local linear regression using techniques from Kolesár and Rothe (2018). Columns 2-4 report the results of estimating the discontinuity at 65 using three parametric models and robust standard errors with linear, quadratic, and cubic age trends, respectively. Columns 2-4 report the results of estimating the discontinuity at 65 using three parametric models and clustering standard errors by age (the running variable) as in Lee and Card (2008) with linear, quadratic, and cubic age trends, respectively. Column 8 reports the results of estimating the discontinuity using the local linear regression model as in Calonico, Cattaneo and Titiunik (2015). The sample includes individuals who were age 55-75 between 2008 and 2017. Credit score data used is from Equifax Riskscore 3.0. See Section 2 for additional details on the outcomes and sample. Source: The financial health outcomes are based on 137,340,577 person-year observations from the New York Fed Consumer Credit Panel / Equifax, 2008-2017.

Appendix Table A2: Location-specific estimates and forecasts for 50 largest CZs

		Per capita		Per newly-insured	
		γ_l^f	RMSE	β_l^f	RMSE
State	CZ	(1)	(2)	(3)	(4)
Arizona	Phoenix	-25	11	-273	180
California	Los Angeles	-29	11	-206	171
California	Sacramento	-17	8	-259	112
California	San Diego	-27	7	-443	158
California	San Francisco	-8	10	-108	176
California	San Jose	-14	12	-243	247
Colorado	Denver	-25	6	-409	87
Connecticut	Bridgeport	-15	3	-272	61
District of Columbia	Washington DC	-22	10	-468	208
Florida	Jacksonville	-42	13	-614	248
Florida	Miami	-62	12	-419	139
Florida	Orlando	-44	13	-472	267
Florida	Port St. Lucie	-58	13	-719	243
Florida	Sarasota	-53	13	-485	256
Florida	Tampa	-53	13	-484	222
Georgia	Atlanta	-43	12	-548	206
Illinois	Chicago	-17	9	-277	159
Indiana	Indianapolis	-41	11	-614	194
Maryland	Baltimore	-23	12	-599	265
Massachusetts	Boston	-14	8	-403	263
Michigan	Detroit	-21	11	-417	242
Michigan	Grand Rapids	-8	12	-106	233
Minnesota	Minneapolis	-3	9	-152	225
Missouri	Kansas City	-40	13	-412	240
Missouri	St. Louis	-30	10	-436	180
Nevada	Las Vegas	-53	12	-591	196
New Hampshire	Manchester	-11	11	-148	194
New Jersey	Newark	-18	7	-221	98
New Jersey	Toms River	-14	10	-280	191
New York	Buffalo	-14	3	-449	62
New York	New York City	-12	6	-197	114
North Carolina	Charlotte	-57	13	-729	268
North Carolina	Raleigh	-53	11	-956	167
Ohio	Cincinnati	-26	9	-456	140
Ohio	Cleveland	-16	10	-281	199
Ohio	Columbus	-37	6	-759	61
Ohio	Dayton	-24	11	-381	208
Oregon	Portland	-10	5	-139	82
Pennsylvania	Philadelphia	-18	6	-344	84
Pennsylvania	Pittsburgh	-21	11	-289	243
Rhode Island	Providence	-2	7	-46	171
Tennessee	Nashville	-52	8	-611	78
Texas	Austin	-43	13	-436	248
Texas	Dallas	-54	13	-502	227
Texas	Fort Worth	-50	12	-563	125
Texas	Houston	-49	12	-435	153
Texas	San Antonio	-43	13	-305	254
Utah	Salt Lake City	-31	13	-276	245
Washington	Seattle	-25	10	-467	213
Wisconsin	Milwaukee	-28	10	-532	215

Note: This table reports the mean square error (MSE)-minimizing forecasts of the reductions in collections debt per capita and the reduction in collections debt per newly-insured for the 50 most populous CZs based on their near-elderly population. We construct the MSE-minimizing forecasting by first running a Lasso regression to predict the CZ-level reductions in collections debt per capita (or per newly-insured). This generates a prediction for each CZ, which we call $\hat{\gamma}_l$. Following Chetty and Hendren (2018) we then combine the $\hat{\gamma}_l$ estimates with our estimates of γ_l to construct the mean square error-minimizing forecast for each commuting zone, γ_l^f, which we present in Column 1. Column 2 presents the root-mean-square error (RMSE) which is calculated using methods from Chetty and Hendren (2018). Column 3 reports the mean square error-minimizing forecast of the reduction in collections debt per newly-insured associated with a (nearly) universal health insurance expansion, β_l^f. Column 4 presents the RMSE for β_l^f. Source: Consumer credit outcomes are based on 137,340,577 person-year observations from the New York Fed Consumer Credit Panel / Equifax, 2008-2017. CZ-level uninsurance rates are from the American Community Survey, 2008-2017. Healthcare market characteristics are from the Healthcare Cost Report Information System (HCRIS) and the Dartmouth Atlas. For details on the data see Section 2.

Appendix Table A3: Description of the Federal Reserve Bank of New York's Equifax Consumer Credit Panel (CCP)

Variable	Description
Amount in collections	the total collection amount of these 3rd party collection accounts.
Number of delinquent accounts	the count of all non-current loans.
Amount delinquent	the sum of all non-current loan balances.
Total credit card balance past due	the difference of total bankcard balance and current bankcard balance.
Total mortgage account balance past due	the difference of total mortgage account balance (incl. home equity installment) and current mortgage balance.
Foreclosure	flag for if an individual recorded a foreclosure in the past 24 months.
New Foreclosure	Number of people that recorded a foreclosure in the current quarter, but not the two previous quarters.
Bankruptcy	flag for if an individual recorded a bankruptcy in the past 24 months.
New Bankruptcy	Number of people that recorded a bankruptcy in the current quarter, but not the two previous quarters.
Equifax Risk Score	always refers to Equifax Risk Score 3.0.

Note: This table reports definitions for the financial variables used from the New York Fed Consumer Credit Panel. The dataset consists of 137,340,577 person-year observations from the New York Fed Consumer Credit Panel / Equifax, 2008-2017.

Appendix Table A4: Correlates with reduction in collections debt at age 65

		Bivariate		Multivariate		Post-Lasso	
Covariate	Estimate Type	Estimate	S.E.	Estimate	S.E.	Estimate	S.E.
Black (%)	Per Capita	-7.17	(2.77)	-5.74	(2.28)	-6.23	(2.08)
Greater than high school education (%)	Per Capita	11.30	(1.74)	-2.47	(3.52)	4.86	(2.46)
Has any coverage (%)	Per Capita	12.00	(1.86)	7.09	(2.94)		
Has Medicaid (%)	Per Capita	6.75	(1.65)	3.24	(2.87)		
Hospital beds per capita	Per Capita	-1.09	(1.4)	1.86	(1.48)		
Income per capita	Per Capita	11.90	(1.79)	6.86	(5.01)		
Median house value	Per Capita	10.70	(1.88)	-2.25	(2.49)		
Hospital occupancy rate (%)	Per Capita	6.56	(1.68)	-0.90	(3.12)		
Physical disability (%)	Per Capita	-11.90	(2)	-5.60	(3.21)	-7.41	(2.56)
Poverty rate (%)	Per Capita	-7.01	(2.34)	-0.01	(3.24)	1.02	(2.16)
Payment by charity care patients ($)	Per Capita	-1.52	(1.65)	-1.78	(1.46)	-2.70	(1.53)
Medicare spending per enrollee ($)	Per Capita	-6.48	(2.08)	-0.63	(2.98)		
For-profit hospitals (%)	Per Capita	-10.20	(1.96)	-4.96	(2.17)	-8.29	(1.97)
Teaching hospitals (%)	Per Capita	9.69	(1.51)	6.14	(3.32)		
Cost of charity care per patient day ($)	Per Capita	0.07	(3.1)	-0.96	(2)	-1.26	(2.21)
Black (%)	Per Newly Insured	-62.20	(37.3)	-54.20	(33.7)	-53.50	(31.8)
Greater than high school education (%)	Per Newly Insured	76.10	(25)	-47.20	(49.8)	-5.16	(39.9)
Has any coverage (%)	Per Newly Insured	-3.87	(29.3)	-127.00	(52.6)		
Has Medicaid (%)	Per Newly Insured	91.80	(28.4)	101.00	(52.8)		
Hospital beds per capita	Per Newly Insured	21.00	(38.2)	46.80	(38.7)		
Income per capita	Per Newly Insured	95.50	(24.9)	125.00	(64.3)		
Median house value	Per Newly Insured	97.20	(30.9)	-58.50	(44.9)		
Hospital occupancy rate (%)	Per Newly Insured	45.20	(34.5)	-6.50	(47.8)		
Physical disability (%)	Per Newly Insured	-113.00	(24.6)	-39.50	(50.8)	-123.00	(38.6)
Poverty rate (%)	Per Newly Insured	-19.30	(28.6)	-66.60	(44.4)	48.80	(26.3)
Payment by charity care patients ($)	Per Newly Insured	-39.30	(33.5)	-38.00	(32.4)	-49.20	(31.5)
Medicare spending per enrollee ($)	Per Newly Insured	-29.50	(32)	-40.20	(45.1)		
For-profit hospitals (%)	Per Newly Insured	-70.00	(28.6)	-65.30	(30.3)	-69.40	(26.6)
Teaching hospitals (%)	Per Newly Insured	110.00	(18.6)	92.70	(55.1)		
Cost of charity care per patient day ($)	Per Newly Insured	29.50	(37.2)	-59.30	(39.1)	0.70	(31.4)

Note: This table reports the CZ-level correlates with our RD estimated reductions in collections debt at age 65 plotted in Figure 3. The "Estimate Type" column indicates whether the row presents correlates with our "per capita" or "per newly-insured" estimates. For each row, we we present the estimates and standard errors for bivariate, multivariate, and post-Lasso models. We standardize all the variables so the coefficients reflect the strength of the association between a one standard deviation change in the covariate and the estimated reduction in collections debt at age 65. The multivariate OLS regression results and post-Lasso multivariate regression results are both run on the full set of characteristics. For post-Lasso, we first estimate a Lasso regression on the full set of characteristics and then report the results of multivariate OLS run on the characteristics chosen by the Lasso regression. Source: Consumer credit outcomes are based on 137,340,577 person-year observations from the New York Fed Consumer Credit Panel / Equifax, 2008-2017. CZ-level uninsurance rates are from the American Community Survey, 2008-2017. Healthcare market characteristics are from the Healthcare Cost Report Information System (HCRIS) and the Dartmouth Atlas. For additional details on the data see Section 2.

Appendix Table A5: Changes in the forecast reductions in collections debt at age 65, pre and post-ACA, used for decomposition in Figure 5

	Per Capita			Insurance Effect			Per Newly Insured			Covariance			Decomposition			
Location	Pre	Post	Diff	Pre	Post	Diff	Pre	Post	Diff	Pre	Post	Diff	η	η_1	η_2	η_3
South	43.61	30.66	-12.95	0.13	0.08	-0.05	365.95	408.95	43.0	-0.95	-0.95	0.00	-0.3	-0.38	0.08	0.00
All Others	14.36	7.23	-7.13	0.09	0.06	-0.04	168.76	167.66	-1.1	0.19	-0.30	-0.49	-0.5	-0.43	0.00	-0.06
Difference	-29.25	-23.43	5.82	-0.03	-0.02	0.01	-197.20	-241.30	-44.1	1.15	0.66	-0.49	-0.2	-0.05	-0.08	-0.06

Note: This table reports the components involved in the decomposition presented in Panel B of Figure 5 and discussed in Appendix B.5. Averages are constructed using unweighted means across commuting zones. South is defined using Census regions, and includes Alabama, Arkansas, Delaware, Florida, Georgia, Kentucky, Louisiana, Maryland, Mississippi, North Carolina, Oklahoma, South Carolina, Tennessee, Texas, Virginia, and West Virginia.